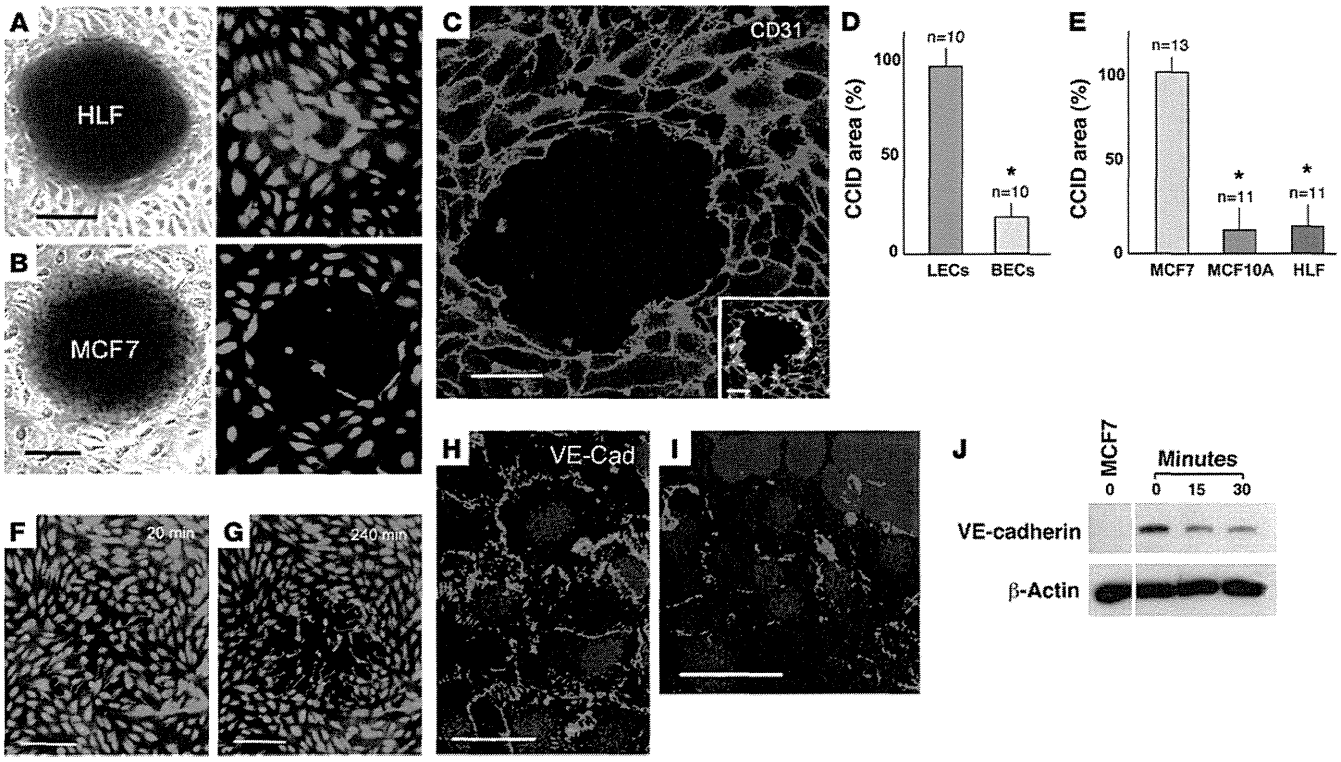

Figure 2

MCF7 cell spheroids induce CCIDs in lymphatic endothelial cell monolayers and disrupt VE-cadherin at the CCIDs. (**A**) Spheroid of HLFs fails to induce any defects in a monolayer of human lymphatic endothelial cells (LECs, Cytotracker tagged in green) after 4 hours of cocultivation. (**B**) MCF7 spheroids induce circular CCIDs. (**C**) A MCF7 spheroid–induced CCID is outlined when the LEC borders are stained for CD31 (red, confocal image). Inset, LECs (demarcated with CD31 in red) at the margin of the CCIDs show expression of PPP1R12A (MYPT1) (green) indicating cell mobility (confocal image). (**D**) MCF7 spheroids induce CCIDs preferentially in LEC monolayers (left bar), but significantly less (14.3% of lymphatics; $^*P = 0.0047$) in monolayers of microvascular blood endothelial cells (BECs, right bar). (**E**) When compared with spheroids of MCF7 cells (left bar, 100%), CCID formation in lymphatic monolayers is marginally induced by nonmalignant human breast epithelial cells MCF-10A (9.6% of MCF7 spheroids), and HLFs (11.3%). Data are presented as mean ± SEM. $^*P < 0.0001$. (**F** and **G**) Tracings of LEC migration (red lines; starting positions are marked by circles) beneath a spheroid during a 4-hour coincubation. (**H**) Confocal image shows continuous LEC junctions of VE-cadherin (VE Cad) at distance from a spheroid. (**I**) At the spheroid's margin, the VE-cadherin pattern is disrupted. (**J**) Confluent LECs were incubated with 1 μM 12(S)-HETE for 15 and 30 minutes or with solvent (0), and cell lysates were immunoblotted with antibodies to VE-cadherin or β-actin. As controls, VE-cadherin$^-$ MCF7 cells were used. Lanes were run on the same gel but are noncontiguous. Scale bars: 100 μm (**A**, **B**, **F**, and **G**); 25 μm (**C**); 50 μm (**H** and **I**).

These results indicated that CCIDs were induced by MCF7 cell spheroids, which were placed onto the upper side of the lymphatic endothelial monolayer that presumably corresponds to the luminal endothelial aspect in vivo. Here we show that CCIDs were also generated when the MCF7 spheroids were placed onto the basolateral aspects of lymphatic endothelial cells in Transwell chambers (Figure 4).

CCIDs were also obtained with spheroids of tumor lines other than MCF7 cells. This was found for human mammary carcinoma cells (HCC1419, HCC1443, and MDA-MB231) and colon cancer (LS174CoCa, HT29, HTC116), melanoma (CRL1675), and pancreatic adenocarcinoma (PANC1) (Figure 3).

Pharmacological inhibition of cognate mechanisms of tumor invasion and metastasis revealed a minor contribution of metalloproteinases since the pan-matrix-metalloprotease inhibitor GM6001 (36, 37), and specific inhibition of MMP9, TIMP2, and MMP2 reduced CCID formation only by approximately 25%. Reactive oxygen species and cyclooxygenases and their products were not involved (Supplemental Table 2).

Inhibition of 15LOX reduces CCID formation in lymphatic monolayers. Further evidence for the central role of *ALOX15* in CCID formation was obtained by shRNA-mediated knockdown in MCF7 cells (MCF7/*ALOX15*$^-$ cells), which resulted in stable reduction of over 80% of *ALOX15* mRNA as well as 12(S)-HETE and 15(S)-HETE production (Figure 5). Nonmalignant human MCF-10A cells or fibroblasts failed to induce CCIDs, to express *ALOX15* and *ALOX12* genes, and to synthesize 12(S)-HETE (Figure 5). Spheroids of MCF7/*ALOX15*$^-$ cells induced small CCIDs that were similar to baicalein-treated MCF7 spheroids, whereas controls (scrambled shRNA or empty vector–transfected MCF7 cells) were similar to unmodified MCF7 cells. This inhibitory effect of *ALOX15* shRNA was further enhanced by the pan-metalloprotease inhibitor GM6001 (Figure 5). Knocking in of *ALOX12* into MCF7/*ALOX15*$^-$ cells (Supplemental Figure 7) fully reestablished their CCID-forming capacity in the spheroid assay (Figure 5).

Reduced metastatic capacity of ALOX15-deficient tumor cells. We used MCF7 cells with transgene expression of VEGFC (MCF7/*VEGFC* cells) (38, 39) to induce metastasis formation in vivo. Both

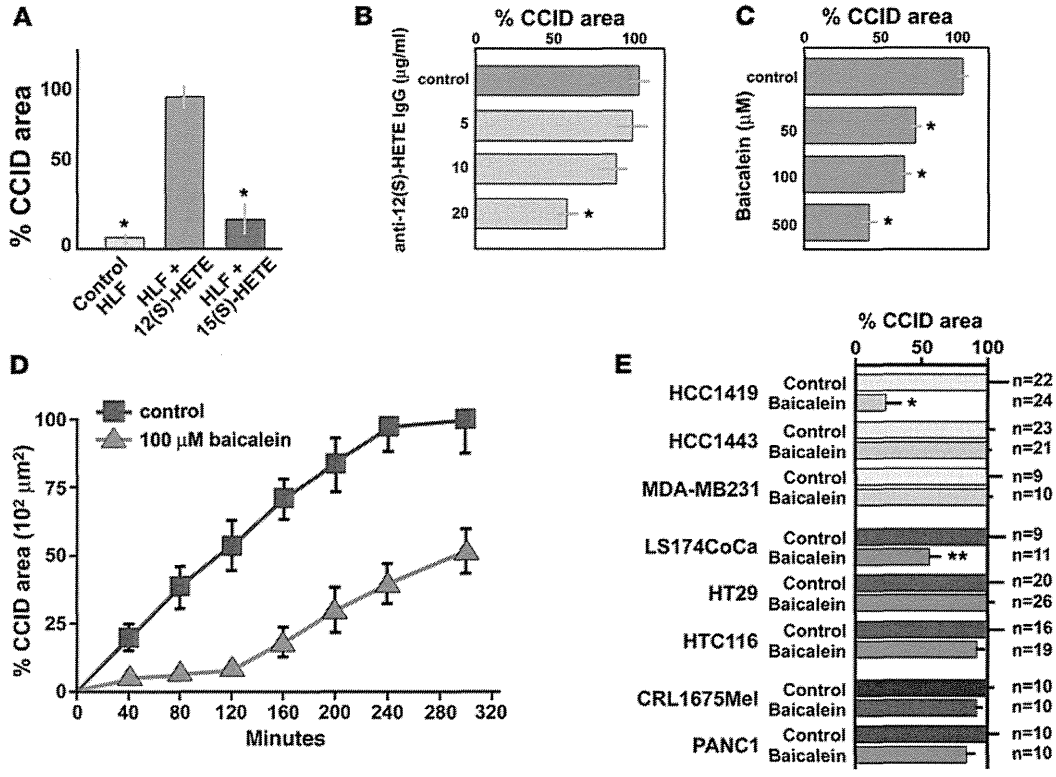

Figure 3

12(S)-HETE causes CCIDs in lymphatic endothelial cell monolayers. (**A**) CCID area in lymphatic endothelial cell monolayers induced by HLF cell spheroids that were presoaked with synthetic 12(S)-HETE ($n = 11$), 15(S)-HETE ($n = 12$), or solvent alone (control; $n = 21$). 12(S)-HETE induced approximately 20 times larger CCIDs than controls ($^*P < 0.0001$) after 4 hours of coincubation. (**B**) Antibody against 12(S)-HETE reduces the CCID area by approximately 50% ($^*P = 0.0020$). (**C**) The ALOX inhibitor baicalein, a traditional Asian anti-cancer drug, reduces CCID area in a dose-dependent fashion, with the highest dose of 500 μM ($n = 11$) causing reduction to 38% ($^*P < 0.0001$) of controls ($n = 20$). (**D**) Time-course incubation over 4 hours with 100 μM baicalein in the media results in approximately 90% reduction of CCID size in the first 2 hours and a gradual increase in CCID formation to more than 50% after 4 hours. (**E**) Spheroids made of the mammary carcinoma cell lines HCC1419, HCC1443, and MDA-MB231 form spheroids that induce CCIDs in lymphatic monolayers, but only HCC1419 cell–mediated CCID formation is sensitive to 100 μM baicalein (inhibition of 78.2%; $^*P = 0.0008$). Similarly, spheroids formed from colorectal carcinoma cell lines LS174CoCa, HT29, and HTC116 form CCIDs, but only LS174CoCa are baicalein sensitive (inhibition of 53.3%; $^{**}P = 0.0168$). A melanoma (CRL1675Mel) and a pancreatic carcinoma cell line (PANC1) formed CCIDs in monolayers of lymphatic endothelial cells, but were insensitive (i.e., statistically not significant) to baicalein. All data are presented as mean ± SEM.

VEGFC-overexpressing and unmodified MCF7 cells expressed *ALOX15* and formed CCIDs of similar size in lymphatic monolayers (Supplemental Figure 8). Stable transfection with luciferase (MCF7/*VEGFC/luc*) did not interfere with the expression of other transgenes (data not shown). MCF7/*VEGFC/ALOX15*$^-$/*luc* or control MCF7/*VEGFC/luc* cells that contained scrambled shRNA were injected orthotopically into mammary fat pads of SCID mice. After 32 days, tumors had formed in 100% of animals injected with control MCF7 cells, but only in 50% with MCF7/*VEGFC/ALOX15*$^-$ cells, presumably due to a less receptive micromilieu at the sites of injection, which showed minimal inflammatory infiltration in all cases. However, once established, the xenograft tumors of all MCF7/*VEGFC* cell variants showed similar growth rates, tumor cell turnover, weights, and intratumoral lymphatic vascular densities (Figure 6). At 32 days, 60% of animals in the control groups, but none of the mice bearing MCF7/*ALOX15*$^-$ xenograft tumors, had developed regional lymph node metastases (Figure 6). Sixty-three days after injection, we found lymph node metastases in 100% of control mice, but only in 5% of the MCF7/*ALOX15*$^-$ group. At this end point, the weight of all primary xenograft tumors was similar, and the expression of *VEGFC* transgene and the *ALOX15* shRNA knockdown were unaltered (Figure 6). In xenograft tumors induced by cells of the *ALOX15*-expressing control groups, podoplanin$^+$ and LYVE1$^+$ intratumoral lymphatic vessels had formed that were distended and focally obliterated by tumor emboli at 32 days after injection (38, 39). In contrast, tumors composed of MCF7/*VEGFC/15LOX*$^-$ cells developed collapsed intratumoral lymphatic vessels that were devoid of embolic tumor cells (Figure 6). These in vivo results support the concept that *ALOX15*-driven production of 12(S)-HETE is required for formation of lymph node metastases, by facilitating the entry of tumor cells into intrametastatic lymphatic vessels.

ALOX15 and 12(S)-HETE in human metastases. The relevance of our experimental findings for the formation of human postsentinel lymph node metastases was underscored by immunohistochemical localization of 12(S)-HETE and of ALOX15 in metastatic carcinoma cells in sentinel lymph nodes (Figure 7). This was extended and confirmed by further analysis of tissue arrays containing cores of primary tumors and their corresponding sentinel metastases from

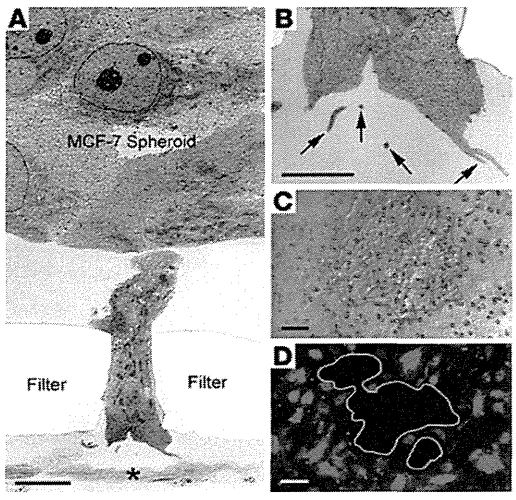

Figure 4
MCF7 tumor cell induced CCID formation in lymphatic monolayers from the abluminal side in Transwell inserts. MCF7 cell spheroids were placed onto the upper side of a filter that was covered by an LEC monolayer on its lower side so that the spheroids were separated from the lymphatic endothelial cells by the filter membrane. Coincubation was performed for 12 hours. (**A**) Low-power electron micrograph of a spheroid extending a "finger" through a filter pore. The LEC monolayer at the basal aspect of the filter shows only extracellular material and debris (*). (**B**) Higher magnification of the tip of the spheroid's extension, showing microvillar or vesicular (arrow) membrane structures, resembling shedding microparticles. (**C**) A spreading spheroid of MCF7 cells (outlined in red) on the upper face of the Transwell membrane. (**D**) At the opposite basal (abluminal) side of the Transwell membrane, a CCID (outlined in green) is formed in the monolayer of lymphatic endothelial cells (tagged red) precisely corresponding to the MCF7 spheroid on the luminal side. Scale bars: 1 μm (**A**); 0.2 μm (**B**); 50 μm (**C** and **D**).

13 patients with ductal carcinomas. These samples were precisely matched for staging pT1c and pN1a. Scoring of immunostaining for ALOX15 (Figure 7) provided evidence for a link between enzyme expression in lymph node metastases and the time of metastasis-free survival, and thus clinical outcome. A similar trend was also observed for the expression of ALOX12 (Supplemental Figure 9).

Discussion

The number of axillary lymph nodes that host metastases of mammary carcinomas is of predictive clinical significance. In this study, we have gained insights into the potential cellular and molecular events involved in metastatic tumor progression from the sentinel to the postsentinel axillary lymph nodes in human mammary carcinomas. This process involves premetastatic conditioning of axillary lymph nodes, invasion of tumor cells into the interconnecting lymphatic vessels, and eventually intranodal tumor cell arrest and proliferation.

Tumors programmed for lymph node metastasis have acquired a specific strategy for premetastatic adaptation of their regional lymph nodes (40, 41), which prominently involves expansion of lymph node sinus and transformation of their lining cells into lymphatic endothelia. This reaction is a stereotypic response to diverse stimuli that range from chemokines and growth factors to lymph congestion by mechanical obliteration of efferent lymphatic vessels (42, 43). However, it is of importance for formation of lymph node metastases and is referred to as *premetastatic lymph node lymphangiogenesis* (41). Moreover, lymphatic vessels develop de novo within the lymph node's metastatic colony and are frequently embolized by tumor cells that phenotypically correspond to cells of the metastasis and not to those in the primary tumors. Intrametastatic lymphangiogenesis occurs in all cases with postsentinel metastasis, and it is also present when the tumor is restricted to the sentinel lymph node. However, only when tumor cells have invaded and embolized the intrametastatic lymphatics do they spread to further lymph nodes downstream, as documented by a 100% correlation of embolization with postsentinel lymph node metastasis, which also applies to further tumor spreading from postsentinel metastases into more distal axillary lymph nodes. This also implies that the intrametastatic lymphatics are connected to the lymph node's efferent lymphatic vessels and is in line with recent experimental evidence (44). Collectively, these results indicate that tumor cell invasion of intrametastatic lymphatic vessels is crucial for lymphatic metastatic tumor dissemination.

These results raise the question of how the tumor cells get access into the intrametastatic lymphatic vasculature. Several pathways of tumor invasion into lymphatic vessels have been observed for different experimental and human tumors (45). One variant implies single tumor cell penetration between or even through endothelial cells, possibly also involving tumor cell epithelial-mesenchymal transition (21, 46, 47). In this investigation, we provide evidence for another pathway for mammary carcinomas similar to that previously described (45), which involves bulk invasion of metastatic tumor cells through large discontinuities of the lymphatic vessel wall. This pathway matches with recent experimental results obtained by in vivo microscopy in which xenografted mammary carcinoma cells spontaneously form mobile cohesive groups that preferentially invade into lymphatic vessels (24).

To gain insights into the mechanisms underlying lymphatic bulk invasion, we have adapted a reductionistic in vitro assay (25, 26) that mimics some features of the in vivo situation. In this system, tumor cell spheroids corresponded to invasive tumor aggregates in vivo, and in lieu of intrametastatic lymphatic vessels, we used monolayers of dermal lymphatic endothelial cells. This choice of endothelial cells was justified because a panel of typical lymphatic genes, including PROX1 and podoplanin, was expressed equally in both normal dermal and intrametastatic lymphatic endothelial cells. In contrast, we have noted that MCF7 cells altered their gene expression program upon spheroid formation and that this includes overexpression of the 12(S)-HETE–producing enzyme ALOX15. The human gene project has revealed 2 *ALOX* isoforms, *ALOX15* and *ALOX15B*. ALOX15B produces 15(S)-HETE only, and there is no evidence that it plays a role in breast cancer pathology (48, 49). In contrast, ALOX15 also generates 12(S)-HETE, which is of relevance for various cancers, including mammary carcinomas (50).

12(S)-HETE was previously shown to increase malignant behavior of some tumors and to reduce it in others (51), and to increase endothelial cell motility and retraction of human umbilical cord endothelial cells (52). This has prompted us to investigate the role of 12(S)-HETE in our in vitro surrogate system of tumor bulk invasion. Our results show that 12(S)-HETE released by MCF7 tumor spheroids induced CCIDs that were formed by centrifugal migration of lymphatic endothelial cells just beneath spheroids. It is possible that this local restriction of endothelial cell mobility could be due to the hydrophobicity

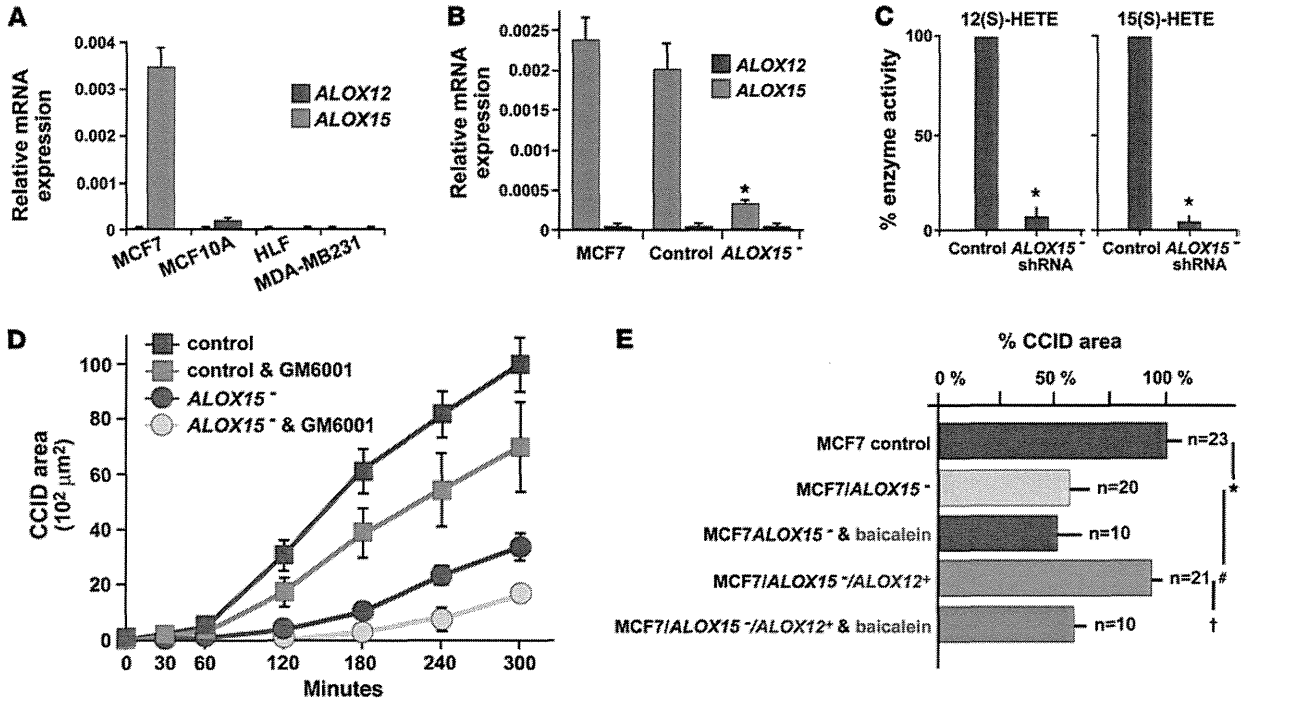

Figure 5

shRNA-mediated knockdown and rescue of lipoxygenase in MCF7 cells. (**A**) The expression of mRNAs of *ALOX15* and *ALOX12* was determined by real-time PCR in MCF7 and MDA-MB231 mammary carcinoma cells and in controls (noncancerous breast epithelial cells MCF-10A and HLFs). MCF7 cells express only *ALOX15* mRNA, but not *ALOX12* mRNA, whereas all other cells fail to produce any of the tested *ALOXs*. (**B**) mRNA levels of *ALOX15* were determined in unmodified MCF7 cells, in control MCF7 cells transduced with scrambled shRNA, and in MCF7/*ALOX15*$^-$ cells. Knockdown of *ALOX15* reduced the expression of *ALOX15* mRNA significantly (*$P = 0.0009$ compared with vector control) when compared with unmodified or control transduced MCF7 cells. (**C**) Production of 12(S)-HETE and 15(S)-HETE, the arachidonic acid metabolites of ALOX15, is reduced by more than 90% in MCF7/*ALOX15*$^-$ cells when compared with control MCF7 cells that were transduced with scrambled shRNA (*$P > 0.0001$). (**D**) shRNA-mediated knockdown of *ALOX15* in MCF7 cells (blue line) causes a size reduction similar to that of baicalein in CCID (compare to Figure 3D). This is further aggravated by coincubation with 20 µM of the pan-metalloprotease inhibitor GM6001 (yellow line), which had a similar effect (green line) on controls (MCF7 cells transduced with scrambled shRNA, red line). (**E**) Reconstitution of CCID-forming activity of MCF7/*ALOX15*$^-$ cells by transfection with *ALOX12*. MCF7 spheroid–induced CCID formation is analyzed in the presence or absence of 100 µM baicalein. There is a significant difference in CCID size between MCF7/control versus MCF7/*ALOX15*$^-$ spheroids (*$P = 0.0017$), MCF7/*ALOX15*$^-$ versus MCF7/*ALOX15*$^-$/*ALOX12*$^+$ spheroids (#$P = 0.0249$), and MCF7/*ALOX15*$^-$/*ALOX12*$^+$ spheroids ± baicalein treatment (†$P = 0.0331$). All data are presented as mean ± SEM.

of 12(S)-HETE that could be released in poorly diffusing membrane microvesicles above its critical micellar concentration (53). However, the actual concentration of 12(S)-HETE in the micromilieu at the spheroid tumor endothelial interface remains to be determined (54). 12(S)-HETE was not toxic for lymphatic endothelial cells, and accordingly, we failed to encounter apoptotic endothelial cells in association with CCIDs. The significance of 12(S)-HETE was confirmed by blocking of CCID formation by a specific antibody or by shRNA-mediated knockdown of the producing enzyme ALOX15. The ability to cause CCIDs was restored by knocking in of *ALOX12*, which also produces 12(S)-HETE and is not expressed in MCF7 cells. 15(S)-HETE, the alternative arachidonic acid metabolite produced by ALOX15, was ineffective. CCID formation was further supported by metalloproteases that loosen the meshwork of VE-cadherin at interendothelial junctions and matrix attachment (36, 37). Taken together, our in vitro findings suggested a hitherto unknown dominant role for ALOX15 and its product 12(S)-HETE in tumor cell–lymphatic endothelial cell interaction. When we extrapolate these in vitro findings to the vascular defects we have observed at sites of tumor cell bulk invasion, it is possible that induction of lymphatic endothelial migration and focal disruption of interendothelial adhesion (e.g., by destabilization of VE-cadherin) could contribute to focal openings in the vascular wall.

Intriguingly, blood endothelial cells were much less sensitive to the migration-inducing effect of 12(S)-HETE than lymphatics. It remains to be determined whether or not this is due to differences in receptor- or nonreceptor-mediated effects. So far, several proteins have been implicated in binding of 12(S)-HETE; however, a definitive universal receptor or receptors are still elusive. We have screened for the expression of 2 putative 12(S)-HETE membrane protein receptors — the leukotriene B_4 receptor (55) and the orphan receptor GPR31 (56) (data not shown) — and failed to detect expression differences between blood and lymphatic endothelial cells. Thus, our results show that 12(S)-HETE preferentially caused CCID formation in lymphatic endothelial monolayers, either by direct interaction with so-far elusive lymphatic receptor or receptors, or indirectly, via currently unidentified intermediaries.

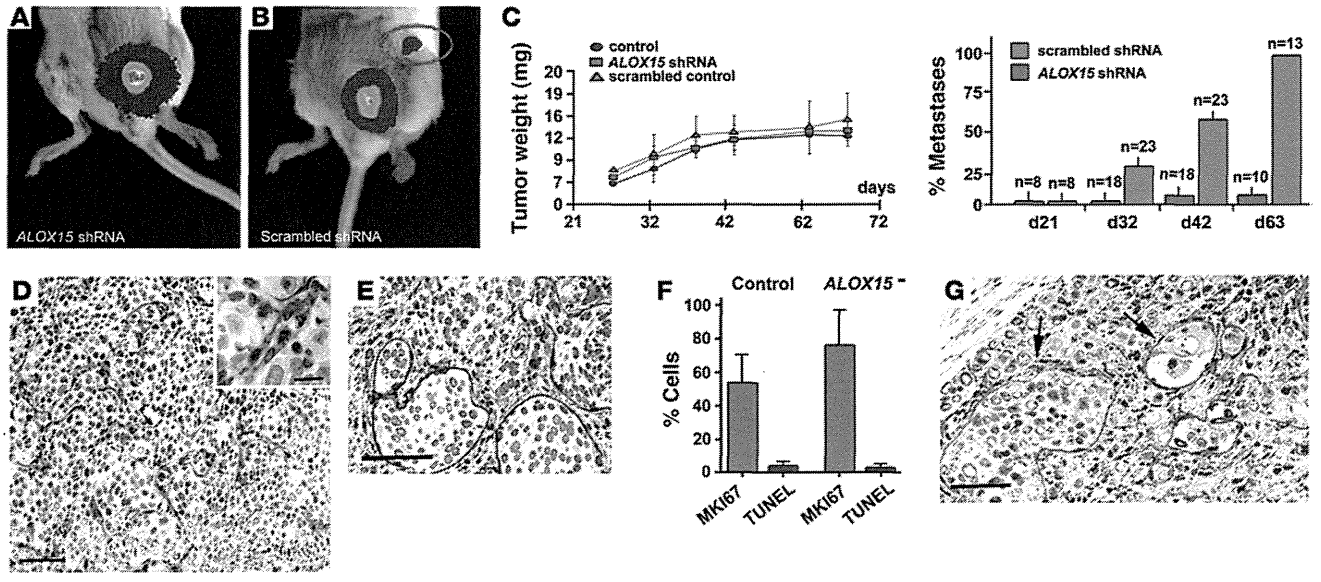

Figure 6

Xenograft tumors induced by *ALOX15* shRNA knockdown cells and control MCF7/*VEGFC* cells expressing luciferase as reporter. (**A**) Bioluminescence image of a xenograft tumor induced by cells that lack *ALOX15* after injection into the fifth mammary fat pad failed to develop lymph node metastases after 32 days. (**B**) Image of a xenograft tumor induced by control MCF7/*VEGFC* cells that were transfected with scrambled shRNA and expressed *ALOX15*, showing a regional lymph node metastasis (red circle). (**C**, left panel) The sizes and growth rates of all xenograft tumors, irrespective of the nature of the inoculated tumor cells (MCF7/*VEGFC*, or MCF7/*VEGFC* cells transfected with scrambled or *ALOX15* shRNA) were similar. (**C**, right panel) Time course of metastasis formation of xenograft tumors induced by MCF7/*VEGFC* cells transfected with *ALOX15* shRNA (red) or with control scrambled shRNA (green) showing that *ALOX15*-deficient MCF7/*VEGFC* were incompetent of metastasis formation. (**D**) Representative picture of a xenograft tumor (same as depicted in **A**). The tumor cells fail to invade into the collapsed intratumoral podoplanin$^+$ lymphatic vessels (red). Insert, tumor embolus–free intratumoral lymphatic vessel with a narrow lumen. (**E** and **G**) Xenograft tumor of the control group (same as in **B**) showing massive tumor intravasation into dilated lymphatic vessels (arrows) that were immunostained for LYVE1 (**E**) or podoplanin (**G**). (**F**) Growth rates of xenograft tumor MCF7/*VEGFC* and MCF7/*VEGFC*/*ALOX15*$^-$ cells were determined by labeling for MKI67 (Ki-67) or by the TUNEL assay. Image analysis revealed a higher (but not significant) MKI67 positivity in *ALOX15*$^-$ tumors compared with control tumors. The rate of apoptosis was similar in both primary tumor types. $n = 6$. Total number of counted nuclei was greater than 2000. Scale bars: 70 μm (**D**, **E**, and **G**); 20 μm (inset). All data are presented as mean ± SEM.

Our results apply primarily to ductal mammary carcinomas that are represented in vitro by MCF7 and HCC1419 cells derived from estrogen receptor–positive ductal carcinomas of the luminal subtype (57). However, only 50% of the lobular mammary carcinomas followed this pattern of tumor spreading. Baicalein-insensitive CCIDs were formed by MDA-MB321 and HCC1443 mammary carcinoma cells that are derived from estrogen receptor–negative ductal carcinomas of the basal subtype and lack ALOXs. This is in contrast to our findings in human tumors and could be due to changes induced by in vitro culturing. Furthermore, the CCID assay suggested that tumors derived from other organs apparently use LOX-independent mechanisms. These include most colorectal carcinomas, melanomas, and a pancreatic cancer. Thus, there is no universal mechanism by which different types of tumors form and propagate lymph node metastases. They apparently also have at their disposal ALOX15-independent mechanisms to enter lymphatic vessels and do not use bulk but rather single-cell invasion, with or without epithelial-mesenchymal transition, possibly depending on TGF-β (24).

These results required verification in a tumor xenograft model that mimics the key findings in sentinel lymph node metastases, i.e., formation of intratumoral lymphatic vessels, bulk invasion of tumor cells, lymphatic embolization, and formation of lymph node metastases. A suitable model for this in vivo proof of principle was found in mouse xenograft tumors produced by human mammary carcinoma MCF7 cells that transgenically overexpress VEGFC (38, 39). This transforms MCF7 cells from nonmetastatic into highly metastatic, with intratumoral lymphangiogenesis, lymph vessel invasion, and embolization, i.e., analogous to human sentinel lymph node metastases. Moreover, we found that MCF7 cells express only a single lipoxygenase, *ALOX15*, and are thus ideally suited for studying the contribution of this enzyme to CCID. shRNA-induced knockdown of *ALOX15* efficiently repressed formation of lymph node metastases. Intratumoral lymphatic vessels were induced both in the control and the *ALOX15* knockdown xenografted tumors. However, in ALOX15-deficient tumors, the lymphatics were collapsed and empty and tumor cells failed to invade and form emboli, in striking contrast to *ALOX15*-expressing and 12(S)-HETE–producing control MCF7 cells. However, we cannot exclude the possibility that the absence of LOX products alters the lymphatic endothelial phenotype to make it less permissive to tumor cell invasion in general.

Here we have brought together 3 correlative observations, i.e., the embolization and invasion of mammary carcinoma cells into intrametastatic lymphatics in human tissues, the 12(S)-HETE–driven formation of CCIDs in vitro, and the important role of the 12(S)-HETE–producing enzyme, ALOX15, for lymph node metastasis formation in mouse xenograft models.

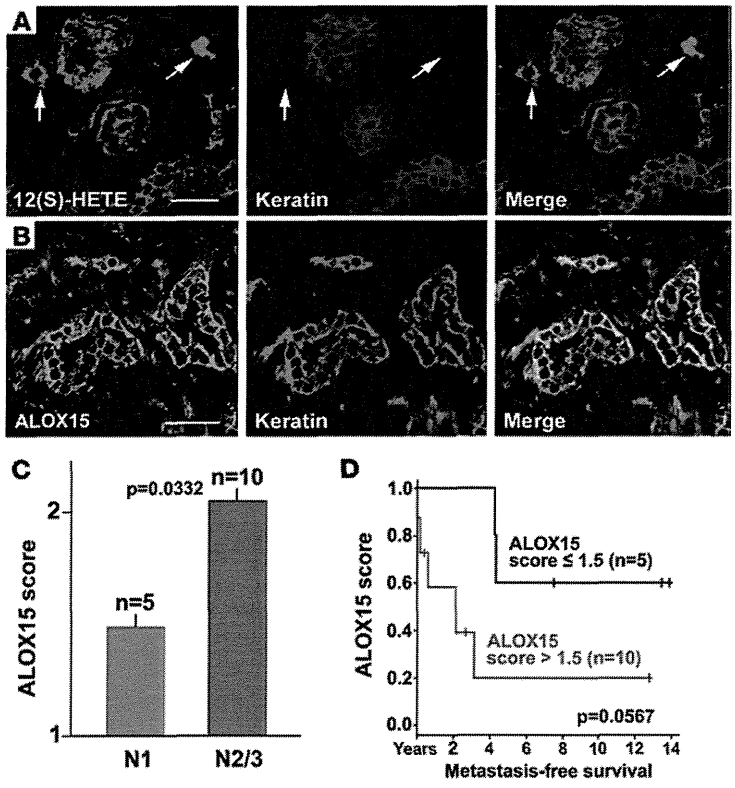

Figure 7
12(S)-HETE and ALOX15 in human sentinel metastases. (**A**) Localization of 12(S)-HETE (red) in the mammary carcinoma cells in a representative sentinel lymph node of a patient with postsentinel lymph node metastasis (total examined: $n = 12$). 12(S)-HETE colocalizes with tumor cell keratin (blue and merge) and is also expressed by nontumor, presumably inflammatory cells (arrows). (**B**) The 12(S)-HETE–producing enzyme ALOX15 shows a localization similar to that of its product (ALOX15: green; keratin: red). (**C**) Results of the tissue array scoring of the immunostaining for ALOX15 in the tumor cells of the sentinel metastasis in 15 cases of ductal carcinoma. In 5 cases without postsentinel metastases, the score is lower (N1, green column) than in 10 cases with postsentinel spreading (N2/3, red column). (**D**) Metastasis-free survival correlates inversely with the expression of ALOX15 in the tumor cells of the sentinel lymph nodes ($P = 0.0507$). Scale bars: 50 μm. All data are presented as mean ± SEM.

Taken together, these complementary results favor the hypothesis that 12(S)-HETE–mediated CCID formation is a central event for accession of mammary carcinoma cells into the lymphatic vasculature in sentinels and thus furthers tumor spreading into postsentinel lymph nodes (Supplemental Figure 10).

Do these potential mechanisms of intrametastatic lymphatic invasion also apply to human patients? Our results suggest that this is feasible. Metastatic tumor cells in sentinel lymph nodes of human mammary carcinomas express all the key players, ALOX12, ALOX15, and 12(S)-HETE. In feasibility studies using tissue microarrays of a relatively small number of carefully matched human samples, we found that the abundance of ALOXs is inversely correlated with metastasis-free survival. Pharmacological ALOX inhibition has previously been recognized as antimetastatic and proapoptotic (58, 59) therapy for mammary and other carcinoma cells. Here we show the CCID-reducing efficiency of the ALOX inhibitor baicalein (34), a polyflavone isolated from the roots of *Scuttelaria baicalensis* and still applied in traditional Asian medicine. Thus, our findings could hold the potential that inhibition of ALOX interferes with lymphatic dissemination of ductal mammary carcinomas. Formal clinical studies are required to determine whether or not ALOXs in mammary carcinomas can be used as biomarkers and potential therapeutic targets.

Methods

Selection of cases and tissue samples. Use of human tissue samples and experimental mouse models was approved by the Ethical Committee of the Medical University of Vienna (Approval EK-Nr 270/2006) in compliance with Austrian legislation. We have selected 104 archival cases of mammary carcinomas, classified as NOS, with 69 cases of ductal and 35 of lobular subtype. The patients had not received preoperative neoadjuvant therapy. The primary tumors were matched by their diameters (pT1c, 1–2 ± 0.6 cm), availability of the sentinel, and, when clinically indicated, also postsentinel axillary lymph nodes. Further inclusion criteria were similar sizes of sentinel lymph node metastases (pN1a, >2 mm) and documented follow-up periods of 55 months after surgery. The tumor grading is listed in Table 1. The tumors were also subclassified by immunohistochemistry as luminal, basal, or ERBB2 enriched (22). Sentinel lymph nodes were free of tumors (stage pN0, $n = 16$) (11), or metastasis was restricted to the sentinel lymph node only (pN1a, $n = 56$), or also involved additional postsentinel axillary lymph nodes (pN2 or 3, $n = 32$). All tumors were analyzed for the expression of estrogen and progesterone receptors, the overexpression of ERBB2, and in some cases also for keratins, CD133, CD44, and aldehyde dehydrogenase (60, 61). As controls, naive nontumor-associated lymph nodes were used that were removed during carotid angioplasty or abdominal surgery ($n = 16$). These nonactivated lymph nodes were devoid of capsular fibrosis, intranodal scars, or activation of germinal centres.

Immunohistochemistry. 4-μm–thick freshly prepared sections from archival paraffin blocks for immunolabeling were processed as described previously (62) using rabbit anti-human podoplanin IgG (5 μg/ml) or with a monoclonal mouse IgG (Bender Med Systems BMS 1105; 1 μg/ml), and anti-human PROX1 rabbit IgG (AngioBio). Some sections were also incubated after podoplanin labeling with monoclonal mouse anti-Ki67 IgG (MIB-1) or anti-human LYVE1 rabbit IgG (DAKO). Rabbit antibodies to 12(S)-HETE (Assay Designs), with less than 2.5% cross-reactivity with 12(R)-HETE and less than 0.3% with 15(S)- and 5(S)-HETE, and ALOX12 and ALOX15 (Abcam) were used on cryostat sections of unfixed primary carcinomas and their sentinel metastases ($n = 12$). For immunofluorescence, we used appropriate secondary antibodies labeled with Alexa Fluor 488, Alexa Fluor 594, or Alexa Fluor 633 (Molecular Probes). Double-labeling experiments were controlled

by omitting the primary antibodies or by replacement with irrelevant antibodies raised in the same species or of the same mouse IgG subtype. The densities of lymphatic vessels were determined in duplicate by 3 independent observers on unmarked histological sections. We counted the number of lymphatic vessel profiles in at least 30 microscopic fields for each slide, using an objective lens with ×25 magnification. Inter- and intra-observer variations resulted in a "background noise" of 1 vessel per field, and only counts above this threshold were entered into the evaluation. Statistical significance was determined by the *t* test, using the Prism 4 software package (GraphPad). Production and composition of tissue microarrays were performed as described (63). We have carefully selected 15 cases of ductal carcinomas with the identical stages pT1c, pN1a (n = 10), and pT1c, pN2/3 (n = 5).

Isolation and characterization of human dermal lymphatic endothelial cells. Human lymphatic endothelial cells and blood vessel endothelial cells were prepared from commercial (C-12260; PromoCell) or freshly prepared dermal microvascular endothelial cells by sorting with anti-podoplanin and anti-CD31 IgG using Dynabeads (M-280; Dynal 11203) or FACS (FaxStar), as described (64). Also, telomerase "immortalized" lymphatic endothelial cells were used (27). No differences in the expression of other proteins previously thought to distinguish lymphatic vessels outside and within tumors (biglycan, endoglin, CD34, VE-cadherin) were found (Supplemental Figure 4C).

Determination of 12(S)-HETE. 12(S)-HETE and 15(S)-HETE were determined by a reverse-phase high-performance liquid chromatography method (RP-HPLC), as described (65).

Spheroid preparation. Cell spheroids were prepared as described in preliminary experiments (25, 26). Briefly, MCF7 cells were grown in McCoy 5A medium containing 10% fetal calf serum and 1% penicillin/streptomycin (Gibco-BRL; Invitrogen). Noncancerous MCF-10A breast epithelial cells were grown in MEGM medium (CC-3150; Clonetic Bullet Kit) supplemented with bovine pituitary extract, human epithelial growth factor, hydrocortisone, insulin, 1% penicillin/streptomycin, and 10 μM isoproterenol. Normal HLFs were grown in nonessential amino acid media containing 10% fetal calf serum and 1% penicillin/streptomycin and 1% nonessential amino acids.

Low-density real-time PCR arrays. Template cDNAs prepared from total RNA of MCF7 cells grown as monolayer or spheroid were characterized in triplicates using the Human Extracellular Matrix and Adhesion Molecules PCR Array (SABiosciences) and the RT2 SYBR Green/Fluorescein qPCR Master Mix (SABiosciences) on the Chromo4 PCR System (Bio-Rad), following the manufacturer's instructions. The resulting Ct values were analyzed by using the RT2 Profiler PCR Array Data Analysis Template v3.2 (SABiosciences). Genes not included on the low-density real-time array were analyzed by using the following FAM probes obtained from Applied Biosystems: *VEGFA* Hs00173626_m1, *ALOX15* Hs00609608_m1, *ALOX12* Hs00167524_m1, and *ALOX12B* Hs00153961_m1.

MCF-7 spheroid/LEC monolayer cocultivation. In all experiments, telomerase-"immortalized" lymphatic endothelial cells (27) or freshly prepared lymphatic endothelial cells (64) (maximal 6 passages) were used, with identical results. Lymphatic endothelial cells were seeded in EGM2MV medium on 24-well plates and allowed to grow to confluence. Then, the lymphatic endothelial cells (LECs) monolayers were stained with Cytotracker green (2 μg/ml, C2925; Molecular Probes) or Hoechst 33258 (5 μg/ml, H1398; Sigma-Aldrich) at 37°C for 90 minutes. Into each well, 10 MCF7 spheroids were transferred. During the coincubation period, frames were taken at 15-minute intervals with an inverse fluorescence microscope (Zeiss Axiophot) and composed to a time-lapse video. Some preparations were examined in a Zeiss confocal fluorescence microscope.

Transwell culture. Primary or telomerase-immortalized lymphatic endothelial cells were grown on the lower surface of Transwell inserts (membrane diameter 6.5 mm; pore size 8 μm, precoated with 10 μg/ml fibronectin; Costar) until confluent. Then lymphatic endothelial cells were stained with Cytotracker as described above, and tumor cell spheroids were placed onto the upper surface. Coculturing was performed for 24 hours, with fluorescence microscopic control of the LEC monolayer every 180 minutes.

Analysis of CCID formation. Areas of LEC monolayers beneath spheroids were photographed in an Axiovert (Zeiss) fluorescence microscope, using the FITC filter to visualize Cytotracker-stained (green) lymphatic endothelial cells, and the area of CCIDs was measured using Axiovision software (Zeiss).

shRNA knockdown of ALOX15. Lentiviral particles containing shRNA targeting the human *ALOX15* mRNA (SHCLNV-NM_001140) and controls with nonsense shRNA (*SHC002V*) were obtained from Sigma-Aldrich. MCF7 cells that transgenically overexpress *VEGFC* (38) were seeded onto 24-well plates, and transduced with 2e5 TU in 250 μl MEM containing 10% FCS and 8 μg polybrene/ml by spin infection at 1500 *g* at 32°C for 90 minutes. After incubation for 12 hours, the cells were reseeded onto 100-mm culture plates and selected with 1 μg/ml puromycin for 1 week. Single-cell colonies were tested for knockdown efficiency by real-time PCR, normalizing gene expression to the housekeeping gene *GAPDH*.

Knockin of ALOX12 cDNA. N-terminal *V5*-tag was fused to the *ALOX12* full-length cDNA. The fusion was constructed by PCR (5′ primer: TCAGATCCGCTAGCGGGCGCCATGGGTAAGCCTATCCCTA-ACCCTCTCCTCGGTCTCGATTCTACGGGCCGCTACCGCATCC-GCGTGGCCA, 3′ primer: GGTGGCGGCGGCCGCTCAGATGGT-GACACTGTTCTCTATGCAGCTGGG) using standard PCR conditions and an *ALOX12*-containing expression plasmid (gift from Brigitte Marian, Cancer Research Institute, Vienna, Austria) as template. The primer pair contained 5′ Nhe-I and 3′ Not-I linkers and the PCR product was directly subcloned into pTag-CFP-N (Evrogen) by replacing CFP with the tagged fusion construct. The resulting vector DNA was controlled by sequencing and proper expression of the target gene by Western blotting with a *V5*-tag antibody (Invitrogen) using total lysates of transfected cells.

Xenograft tumors. For xenografting, 10^7 MCF7 cells or their derivatives were dispersed in 30 μl PBS and injected orthotopically into the fat pads of the fifth mammary glands of 8-week-old female SCID mice (Harlan Animal Research Laboratory). 60-day slow-release pellets containing 0.72 mg of 17β-estradiol (Innovative Research of America) were implanted 48 hours previously. Primary tumor growth and formation of metastases were monitored at 10-day intervals by noninvasive bioluminescence imaging using a highly sensitive CCD camera (IVIS 100; Caliper Life Sciences). 150 μg D-luciferin/g of body weight (firefly, potassium salt; Caliper Life Sciences) was injected intraperitoneally. Bioluminescence signals were acquired 18 minutes after application, and normalized signals (photons/sec/cm²/sr) were evaluated and quantified using Living Image Software (Caliper Life Sciences); the tumor weight was calculated from a calibration curve. The experiment was terminated after 63 days, and primary tumors and lymph node metastases were processed for anti-podoplanin immunohistochemistry or for mRNA determination of *VEGFC*, *ALOX12*, and *ALOX15*, shRNAs, and luciferase. Paraffin sections of formalin-fixed tissues were labeled by the TUNEL assay (Chemicon), MKI67 (KI-67, Novo Castra NCL-Ki67p), and cytokeratin (DAKO Z0622). Fluorescence microscopy was performed on an Axiophot microscope equipped with an AxioCam Colour camera (Zeiss) at a standard magnification of 250. Images were analyzed using ImageJ software package 1.42q (Wayne Rasband, NIH; http://rsb.info.nih.gov/ij).

Statistics. We have used a 2-tailed *t* test for statistical analysis of the experimental data. $P \leq 0.05$ was considered significant. All data are presented as mean ± SEM. The human correlative data were expressed by Kaplan-Meier statistics.

Acknowledgments

This work was supported in part by European Community project LSHG-CT-2004-503573 (Lymphangiogenomics) (to D. Kerjaschki and K. Alitalo); a research fund from the Keyaki-kai Medical Corporation, Tokyo, Japan (to H. Nosaka); by the GenAU project Drug Action by Genomic Networks (DRANGON) (to V. Sexl); by Fonds für Innovative und Interdisziplinäre Krebsforschung der Gemeinde Wien (to G. Krupitza); and by the Austrian Breast and Colorectal Cancer Study Group (ABCSG) (to M. Gnant and M. Rudas). We thank A. Rees for reading the manuscript and A. Jaeger for help with the graphic work.

Received for publication August 13, 2010, and accepted in revised form February 2, 2011.

Address correspondence to: Dontscho Kerjaschki, Clinical Department of Pathology, Allgemeines Krankenhaus Wien, Medical University of Vienna; Waehringer Guertel 18-20, A 1090 Vienna, Austria. Phone: 431.40400.5176; Fax: 431.40400.5193; E-mail: dontscho.kerjaschki@meduniwien.ac.at.

Gregor Bartel's present address is: Department of Internal Medicine III, Medical University of Vienna, Vienna, Austria.

Veronika Sexl's present address is: Department of Pharmacology, Veterinary Medical University, Vienna, Austria.

Hitonari Nosaka's present address is: Department of Internal Medicine, Teikyo University, Tokyo, Japan.

Monika Hämmerle's present address is: Department of Pathology, University of Heidelberg, Heidelberg, Germany.

Helmut Dolznig's present address is: Department of Medical Genetics, Medical University of Vienna, Vienna, Austria.

1. Fidler IJ. The pathogenensis of cancer metastasis: the "seed-and-soil" hypothesis revisited. *Nat Rev Cancer.* 2003;3(6):453–458.
2. Psaila B, Lyden D. The metastatic niche: adapting the foreign soil. *Nat Rev Cancer.* 2009;9(4):285–293.
3. Metha P. Potential role of platelets in the pathogenesis of tumor metastasis. *Blood.* 1984;63(1):55–63.
4. Tammela T, Alitalo K. Lymphangiogenesis: Molecular mechanisms and future promise. *Cell.* 2010; 140(4):460–476.
5. Eyles J, et al. Tumor cells disseminate early, but immunosurveillance limits metastatic outgrowth, in a mouse model of melanoma. *J Clin Invest.* 2010;120(6):2030–2039.
6. Müller-Hermelink N, et al. TNFR1 signaling and IFN-gamma signaling determine whether T-cells induce tumor dormancy or promote multistage carcinogenesis. *Cancer Cell.* 2008;13(6):507–518.
7. Tait CR, Dodwell D, Horgan K. Do metastases metastasize? *J Pathol.* 2004;203(1):515–518.
8. Norton L, Massagué J. Is cancer a disease of self-seeding? *Nat Med.* 2006;12(8):875–878.
9. Ben-Porath I, et al. An embryonic stem cell-like gene expression signature in poorly differentiated aggressive human tumors. *Nat Genet.* 2008; 40(5):499–507.
10. Carlson RW, et al. Breast cancer. Clinical practice guidelines in oncology. *J Natl Compr Canc Netw.* 2009;7(2):122–192.
11. Sobin LH, Gospodarowicz MK, Wittekind C, eds. *TNM Classification of Malignant Tumours (Uicc International Union Against Cancer).* New York, New York, USA: Wiley-Blackwell; 2009.
12. Britton TB, Solanki CK, Pinder SE, Mortimer PS, Peters AM, Purushotham AD. Lymphatic drainage pathways of the breast and the upper limb. *Nucl Med Commun.* 2009;30(6):427–430.
13. Van den Eynden G, et al. Increased sentinel lymphnode lymphangiogenesis is associated with non-sentinel axillary lymph node involvement in breast cancer patients with a positive sentinel node. *Clin Cancer Res.* 2007;13(18 pt 1):5391–5397.
14. Breiteneder-Geleff S, et al. Angiosarcomas express mixed endothelial phenotypes of blood and lymphatic capillaries: podoplanin as a specific marker for lymphatic endothelium. *Am J Pathol.* 1999;154(2):385–394.
15. Banerji S, et al. LYVE1, a new homologue of the CD44 glycoprotein, is a lymph-specific receptor for hyaluronan. *J Cell Biol.* 1999;144(4):789–801.
16. Wigle JT, Oliver G. Prox1 function is required for the deveLOXpment of the murine lymphatic system. *Cell.* 1999;98(6):769–778.
17. Marinho VF, Metze K, Sanches FS, Rocha GF, Gobbi H. Lymph vascular invasion in invasive mammary carcinomas identified by the endothelial lymphatic marker D2-40 is associated with other indicators of poor prognosis. *BMC Cancer.* 2008;8:64.
18. Van den Eynden GG, et al. Induction of lymphangiogenesis in and around axillary lymph node metastases of patients with breast cancer. *Br J Cancer.* 2006;95(10):1362–1366.
19. Hirakawa S, Kodama S, Kunstfeld R, Kajiya K, Brown LF, Detmar M. VEGFA induces tumor and sentinel lymph node lymphangiogenesis and promotes lymphatic metastasis. *J Exp Med.* 2005;201(7):1089–1099.
20. Schoppmann SF, et al. Tumor-associated macrophages express lymphatic endothelial growth factors and are related to peritumoral lymphangiogenesis. *Am J Pathol.* 2002;161(3):947–956.
21. Hirakawa S, et al. Nodal lymphangiogenesis and metastasis: Role of tumor-induced lymphatic vessel activation in extramammary Paget's disease. *Am J Pathol.* 2009;175(5):2235–2248.
22. Sotiriou C, et al. Breast cancer classification and prognosis based on gene expression profiles from a population-based study. *Proc Natl Acad Sci U S A.* 2003;100(18):10393–10398.
23. Bertucci F, et al. Lobular and ductal carcinomas of the breast have distinct genomic and expression profiles. *Oncogene.* 2008;27(40):5359–5372.
24. Giampieri S, Manning C, Hooper S, Jones L, Hill CS, Sahai E. Localized and reversible TGFbeta signalling switches breast cancer cells from cohesive to single cell motility. *Nat Cell Biol.* 2009; 11(11):1287–1296.
25. Offner FA, et al. Interaction of human malignant melanoma tumor spheroids with endothelium and reconstituted basement membrane: modulation by RGDS. *Int J Cancer.* 1993;54(3):506–512.
26. Madlener S, et al. Multifactorial anticancer effects of digalloyl-resveratrol encompass apoptosis, cell cycle arrest, and inhibition of lymphendothelial gap formation in vitro. *Br J Cancer.* 2010;102(9):1361–1370.
27. Schoppmann SF, et al. Telomerase-immortalized lymphatic and blood vessel endothelial cells are functionally stable and retain their lineage specificity. *Microcirculation.* 2004;11(3):261–269.
28. Matsumura F, Hartshorne DJ. Myosin phosphatase target subunit: Many roles in cell function. *Biochem Biophys Res Commun.* 2008;369(1):149–156.
29. Hultén LM, et al. 15-Lipoxygenase-2 is expressed in macrophages in human carotid plaques and regulated by hypoxia-inducible factor-1alpha. *Eur J Clin Invest.* 2010;40(1):11–17.
30. Funk CD. The molecular biology of mammalian lipoxygenases and the quest for eicosanoid functions using lipoxygenase-deficient mice. *Biochim Biophys Acta.* 1996;1304(1):65–84.
31. Subbarayan V, et al. Inverse relationship between 15-lipoxygenase-2 and PPAR-gamma gene expression in normal epithelia compared with tumor epithelia. *Neoplasia.* 2005;7(3):280–293.
32. Honn KV, et al. Tumor cell-derived 12(S)-hydroxyeicosatetraenoic acid induces microvascular endothelial cell retraction. *Cancer Res.* 1994; 54(2):565–574.
33. Funk CD. Lipoxygenase pathways as mediators of early inflammatory events in atherosclerosis. *Arterioscler Thromb Vasc Biol.* 2006;26(6):1204–1206.
34. Li-Weber M. New therapeutic aspects of flavones: the anticancer properties of Scutellaria and its main active constituents Wogonin, Baicalein and Baicalin. *Cancer Treat Rev.* 2009;35(1):57–68.
35. González-Núñez D, Claria J, Rivera F, Poch E. Increased levels of 12(S)-HETE in patients with essential hypertension. *Hypertension.* 2001;37(2):334–338.
36. Deryugina EI, Quigley JP. Matrix metalloproteinases and tumor metastasis. *Cancer Metastasis Rev.* 2006;25(1):9–34.
37. Baker AH, Edwards DR, Murphy G. Metalloproteinase inhibitors: biological actions and therapeutic opportunities. *J Cell Sci.* 2002;115(pt 19):3719–3727.
38. Karpanen T, et al. Vascular endothelial growth factor C promotes tumor lymphangiogenesis and intralymphatic tumor growth. *Cancer Res.* 2001;61(5):1786–1790.
39. He Y, et al. Vascular endothelial cell growth factor receptor 3-mediated activation of lymphatic endothelium is crucial for tumor cell entry and spread via lymphatic vessels. *Cancer Res.* 2005;65(11):4739–4746.
40. Ran S, Volk L, Hall K, Flister MJ. Lymphangiogenesis and lymphatic metastasis in breast cancer. *Pathophysiology.* 2010;17(4):229–251.
41. Mumprecht V, Detmar M. Lymphangiogenesis and cancer metastasis. *J Cell Mol Med.* 2009; 13(8A):1405–1416.
42. Steinmann G, Földi E, Földi M, Rácz P, Lennert K. Morphologic findings in lymph nodes after occlusion of their efferent lymphatic vessels and veins. *Lab Invest.* 2009;47(1):43–50.
43. Angeli V, et al. B cell-driven lymphangiogenesis

in inflamed lymph nodes enhances dendritic cell mobilization. *Immunity.* 2006;24(2):203–215.
44. Harrell MI, Iritani BM, Ruddell A. Tumor-induced sentinel lymph node lymphangiogenesis and increased lymph flow precede melanoma metastasis. *Am J Pathol.* 2007;170(2):774–786.
45. Carr I. Lymphatic metastasis. *Cancer Metastasis Rev.* 1983;2(3):307–317.
46. Azzali G. Tumor cell transendothelial passage in the absorbing lymphatic vessel of transgenic adenocarcinoma mouse prostate. *Am J Pathol.* 2007;170(1):334–346.
47. Yang J, et al. Twist, a master regulator of morphogenesis, plays an essential role in tumor metastasis. *Cell.* 2004;117(7):927–939.
48. Tang DG, Bhatia B, Tang S, Schneider-Broussard R. 15-lipoxygenase 2 (15-LOX2) is a functional tumor suppressor that regulates human prostate epithelial cell differentiation, senescence and growth (size). *Prostaglandins Other Lipid Mediat.* 2007;82(1–4):135–146.
49. Brash AR, Boeglin WE, Chang MS. Discovery of a second 15S-lipoxygenase on humans. *Proc Natl Acad Sci U S A.* 1997;94(12):6148–6152.
50. Jiang WG, Douglas-Jones A, Mansell RE. Levels of expression of lipoxygenases and cycloxygenase 2 in human breast cancer. *Prostaglandins Leukot Essent Fatty Acids.* 2003;69(4):275–281.
51. Bhattacharya S, Mathew G, Jayne DG, Pelengaris S, Khan M. 15-lipoxygenase-1 in colorectal cancer: a review. *Tumour Biol.* 2009;30(4):185–199.
52. Honn KV, et al. Enhanced endothelial cell retraction mediated by 12(S)-HETE: a proposed mechanism for the role of platelets in tumor cell metastasis. *Exp Cell Res.* 1994;210(1):1–9.
53. Uchide K, Sakon M, Ariyoshi H, Nakamori S, Tokunaga M, Monden M. Cancer cells cause vascular endothelial cell (vEC) retraction via 12(S)HETE secretion; the possible role of cancer cell derived microparticle. *Ann Surg Oncol.* 2007;14(2):862–868.
54. Moreno JJ. New aspects of the role of hydroxyeicosatetraenoic acids in cell growth and cancer development. *Biochem Pharmacol.* 2009;77(1):1–10.
55. Kim GY, Lee JW, Cho SH, Seo JM, Kim JH. Role of the low-affinity leukotriene B4 receptor BLT2 in VEGF-induced angiogenesis. *Arterioscler Thromb Vasc Biol.* 2009;29(6):915–920.
56. Guo Y, Nie D, Honn KV. Cloning and identification of a G-protein coupled receptor for 12(S)-HETE. *Proc Amer Assoc Cancer Res.* 2004;45:2746.
57. Neve RM, et al. A collection of breast cancer cell lines for the study of functionally distinct cancer subtypes. *Cancer Cell.* 2006;10(6):515–527.
58. Umezawa K. Inhibition of experimental metastasis by enzyme inhibitors from microorganisms and plants. *Adv Enzyme Regul.* 1996;36:267–81.
59. Tong WG, Ding XZ, Adrian TE. The mechanisms of lipoxygenase inhibitor-induced apoptosis in human breast cancer cells. *Biochem Biophys Res Commun.* 2002;296(4):942–948.
60. Russo J, et al. The concept of stem cell in the mammary gland and its implication in morphogenesis, cancer and prevention. *Front Biosci.* 2006; 11:151–172.
61. Charafe-Jauffret E, Monville F, Ginestier C, Dontu G, Birnbaum D, Wicha MS. Cancer stem cells in breast: current opinion and future challenges. *Pathobiology.* 2008;75(2):75–84.
62. Wick N, et al. Lymphatic precollectors contain a novel, specialized subpopulation of podoplanin low, CCL27-expressing lymphatic endothelial cells. *Am J Pathol.* 2008;173(4):1202–1209.
63. Vinatzer U, et al. Expression of HER2 and the coamplified genes GRB7 and MLN64 in human breast cancer: quantitative real-time reverse transcription-PCR as a diagnostic alternative to immunohistochemistry and fluorescence in situ hybridization. *Clin Cancer Res.* 2005;11(23):8348–8357.
64. Kriehuber E, et al. Isolation and characterization of dermal lymphatic and blood endothelial cells reveal stable and functionally specialized cell lineages. *J Exp Med.* 2001;194(6):797–808.
65. Werz O, Steinhilber D. Selenium-dependent peroxidases suppress 5-lipoxygenase activity in B-lymphocytes and immature myeloid cells. The presence of peroxidase-insensitive 5-lipoxygenase activity in differentiated myeloid cells. *Eur J Biochem.* 1996;242(1):90–97.

Journal of Dermatological Science 61 (2011) 85–93

Contents lists available at ScienceDirect

Journal of Dermatological Science

journal homepage: www.elsevier.com/jds

Invited review article

Regulation of pathological lymphangiogenesis requires factors distinct from those governing physiological lymphangiogenesis

Satoshi Hirakawa [a,b,*]

[a] Department of Dermatology, Ehime University Graduate School of Medicine, Japan
[b] Department of Cell Growth and Tumor Regulation, Ehime Proteo-Medicine, Research Center, Ehime University, Ehime, Japan

ARTICLE INFO

Article history:
Received 22 October 2010
Received in revised form 22 November 2010
Accepted 30 November 2010

Keywords:
Angiogenesis
Metastasis
Tumor progression
Vascular endothelial growth factor
Vascular development

ABSTRACT

Physiological lymphangiogenesis requires key factors such as vascular endothelial growth factor (VEGF)-C and the homeodomain transcription factor Prox1 to induce the formation of primitive lymph sacs from veins during mammalian development. However, pathological lymphangiogenesis, defined as new lymphatic vessel growth resulting from pathogenic stimuli, may utilize additional signaling pathways and/or cell types in conditions such as tumor progression or inflammatory responses. In fact, although both physiological and pathological lymphatic vascular development share fundamental mechanisms, pleiotropic growth factors and/or pro-inflammatory cytokines mediate lymphangiogenesis in experimental models of pathologic lymphangiogenesis. This review summarizes molecular mechanisms underlying lymphangiogenesis in pathological conditions and focuses in particular on current findings relevant to tumor-associated lymphangiogenesis.

Contents

1. Introduction

Lymphatic vessels give rise to the lymphatic system in conjunction with lymph nodes to facilitate effective immune surveillance in the mammalian body. This structure allows lymphatic vessels to drain lymph, the interstitial fluid in peripheral organs, to the blood circulation [1]. However, pathological conditions such as tumor progression induce new lymphatic vessel growth within primary tumor sites and promote enhanced metastasis to draining lymph nodes [2–4]. Such tumor-associated lymphangiogenesis was first described in 2001 [2–5]. Since then, numerous experimental models and relevant human disease conditions have been analyzed in investigations of pathological lymphangiogenesis. On the other hand, key mechanisms underlying physiological lymphangiogenesis have been identified [1,6–8]. Functional studies of the homeodomain transcription factor Prox1 showed that lymphatic vessels originate from veins during mammalian embryonic development [9,10]. Furthermore, vascular

Abbreviations: COUP-TFII, chicken ovalbumin upstream promoter transcription factor; EMT, epithelial–mesenchymal transition; ESAM, endothelial specific adhesion molecule; LEC, lymphatic endothelial cell; LYVE-1, lymphatic vessel endothelial hyaluronan receptor-1; CLEC-2, C-type lectin-like receptor 2; EMPD, extramammary Paget's disease; M-CSF, macrophage colony-stimulating factor; SCC, squamous cell carcinoma; TGF-β, transforming growth factor-β; TNF-α, tumor necrosis factor-α; VEGF, vascular endothelial growth factor.

* Correspondence address: Department of Dermatology, Ehime University Graduate School of Medicine, Shitsukawa, Toon, Ehime 791-0295, Japan.
Tel.: +81 89 960 5350; fax: +81 89 960 5352.
E-mail address: satoshi2@m.ehime-u.ac.jp.

0923-1811/$36.00
doi:10.1016/j.jdermsci.2010.11.020

endothelial growth factor (VEGF)-C, a key growth factor in physiological lymphangiogenesis, was found to promote activation of VEGFR-3, a receptor tyrosine kinase expressed in lymphatic endothelium [11,12]. Inactivation of genes encoding either *Prox1* or *vegf-c* in mouse promotes loss of lymph sacs, the primitive organs for lymphatic vessels [9,13].

Physiological and pathological lymphangiogenesis likely share certain biological mechanisms. However, substantial evidence indicates that pathological lymphatic vessel growth requires additional factors. Cell types such as inflammatory cells, bone-marrow-derived progenitors, and/or tumor cells, which produce pleiotropic growth factors, pro-inflammatory cytokines, and/or chemokines, are recruited in pathological conditions. These molecules likely alter the structure and function of lymphatic vessels and contribute the pathogenesis of cutaneous diseases. The author has a long-term interest in tumor-associated lymphangiogenesis and the translation of basic research to clinical settings [14–17]. Therefore, this article will review events in tumor lymphangiogenesis and focus on pathological lymphangiogensis in comparison with physiological lymphangiogenesis.

2. Lymphatic vessels as a vital network in the mammalian vascular system

Lymphatic vessels are distributed to most organs including the skin, although some organs such as brain or bone are devoid of lymphatic vessels. Cutaneous lymphatic vessels consist of a dense network that begins by blunt end (Fig. 1, arrowheads). These thin-walled capillary-sized vessels are called 'initial lymphatics' and drain to collecting lymphatic vessels [18]. Furthermore, lymphatic vessels are composed of both peripheral lymphatics and the lymphatic trunk. These vessels communicate with each other to drain lymph into the systemic circulation. Lymphatic vessels have two major functions. One is to absorb and transport interstitial fluids and macromolecules that arise in the extracellular space of peripheral tissues. Lymphatic capillaries absorb interstitial fluid, whereas collecting lymphatics transport the protein-rich lymph to the proximal site. Subsequently, the thoracic duct, a major lymphatic trunk, drains to the venous circulation around the left subclavian or left branchiocephalic vein. The other function of lymphatic vessels is to promote chemo-attraction of immune cells for immune surveillance.

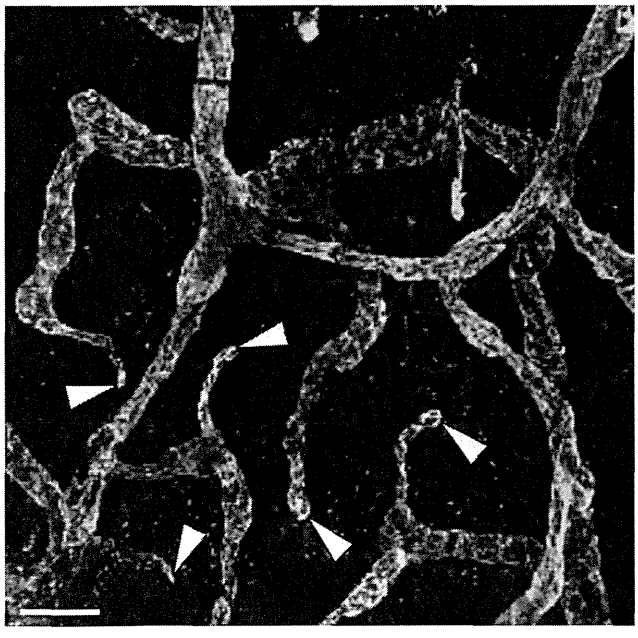

Fig. 1. LYVE-1 is a specific marker of lymphatic capillaries in mouse skin. Double immunofluorescence for LYVE-1 (red) and podoplanin (green). The podoplanin-positive vascular network indicates lymphatic vessels in the skin. Among them, initial lymphatic vessels beginning with a blunt ending (arrowheads) are positive for both LYVE-1 and podoplanin (merge), indicating that LYVE-1 is a marker of lymphatic capillaries. Scale bar: 100 μm.

Recent experimental studies demonstrate that lymphatic vessels play a crucial role in the pathogenesis of hypertension or obesity and undergo major alterations associated with circulatory factors or fat metabolism [19,20]. A high salt diet induces not only hypertension but also sodium accumulation in the skin. A recent study in rats showed that hypertonic stimuli induce cutaneous lymphatic vessel growth though activation of macrophages [20]. The newly formed lymphatic vessels control dermal extracellular volume by efficiently draining interstitial fluid and electrolytes into the circulation. Thus, lymphatic vessels regulate interstitial volume balance and blood pressure, providing a buffering system against experimentally-induced hypertension. Insufficient development of lymphatic vessels also causes adult-onset obesity in *Prox1*-heterozygous mice, which exhibit reduced Prox1 levels [19]. This condition likely results from abnormal leakage from poorly patterned or ruptured lymphatic vessels, promoting lymph accumulation in adipose tissue. A recent study further showed that a high fat diet induces macroscopic swelling and lipid accumulation in the skin of mice with hypercholesterolemia due to apolipoprotein-E deficiency [21]. Furthermore, these mice show markedly enlarged initial lymphatic vessels, and impaired pericyte coverage and valve formation, leading to decreased drainage and abnormal leakage by lymphatic vessels. These findings indicate a close association between fat metabolism and lymphatic vessel function.

3. Establishment of lymphatic-vessel specific markers

Recent progress in understanding lymphatic vascular development and pathology was facilitated by discovery of molecules specifically expressed in lymphatic vessels. In particular, antibodies against lymphatic vessel-specific glycoproteins such as podoplanin or the lymphatic vessel endothelial hyaluronan receptor-1 (LYVE-1) have been widely used to identify lymphatic vessels in physiological and pathological conditions. LYVE-1, a member of the link protein superfamily, was originally identified as a CD44 homologue [22]. LYVE-1 is expressed by lymphatic endothelial cells and is highly specific for lymphatic capillaries (Fig. 1, merge). In the skin, the first lymphatic vessels appear LYVE-1-positive capillaries (Fig. 1). LYVE-1 is one of the most useful markers to visualize lymphatic vessels in mouse experimental models such as that of chemically-induced skin carcinogenesis (Fig. 2C). Loss-of-function studies, however, reveal no specific phenotypes in LYVE-1 null mice [23,24]. In contrast, another study shows that functional inactivation of LYVE-1 in mice resulted in enlargement of capillary-sized lymphatic vessels and in constitutively increased interstitial-lymphatic flow. Therefore, conclusive proof of detailed function in LYVE-1 remains controversial [25]. Another marker of lymphatic vessels, podoplanin, is a sialomucin-type glycoprotein originally identified on the surface of podocytes in rat glomeruli [26]. Podoplanin shows differential expression in cutaneous lymphatic capillaries and collectors from blood vessels (Fig. 1, green). D2-40, a monoclonal antibody recognizing podoplanin, is widely used to diagnose human skin diseases (Fig. 3C). Of note, double staining for podoplanin and Prox1 defines lymphatic vessels, even in pathological conditions such as tumor progression (Fig. 3D). NZ-1, another monoclonal rat IgG against podoplanin, has been used to identify lymphatic vessels in several types of human skin tumors, such as cutaneous malignant melanoma [27]. Recent loss-of-function studies demonstrate that

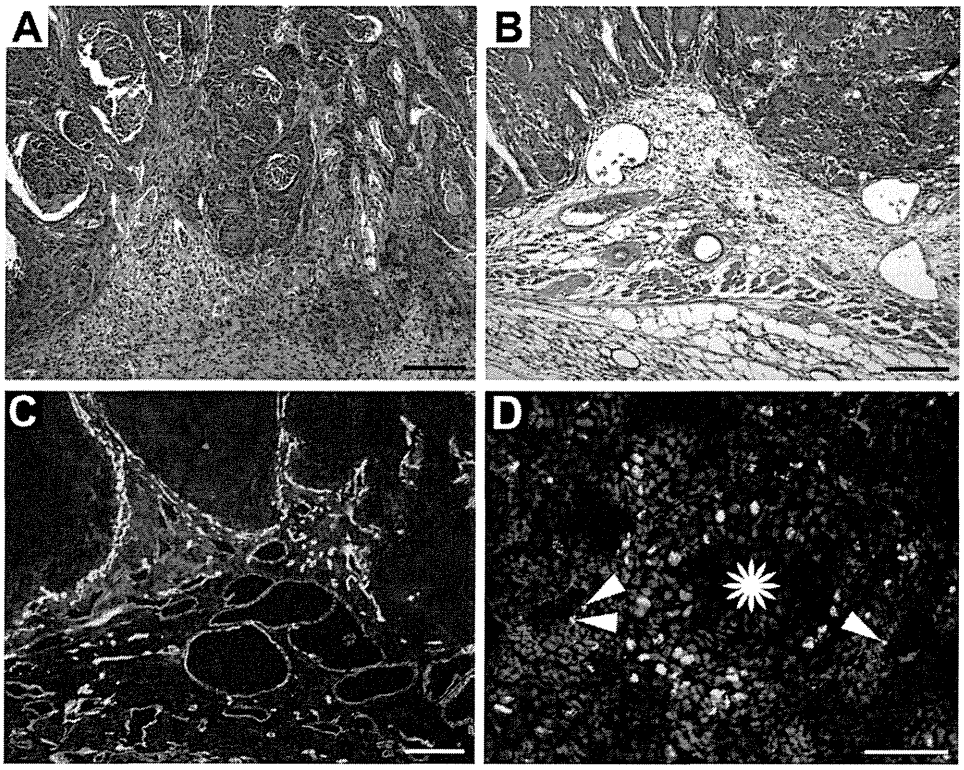

Fig. 2. Targeted VEGF-A overexpression enhances edema formation and tumor lymphangiogenesis in chemically-induced mouse skin carcinogenesis. (A) and (B) Invasive front of squamous cell carcinomas in wild-type mice (A) or Keratin 14-promoter-driven VEGF-A transgenic mice (B). Note that stromal edema is prominent in VEGF-A-overexpressing SCCs compared with controls. (C) Double immunofluorescence for CD31 (green) and LYVE-1 (red) shows marked enlargement of tumor-associated blood and lymphatic vessels in VEGF-A-overexpressing SCCs. (D) Double immunofluorescence staining for BrdU (green) and LYVE-1 (red) shows active proliferation of tumor-associated lymphatic endothelial cells (arrowheads) surrounding tumor nests overexpressing VEGF-A (asterisk), indicating that VEGF-A is a potent lymphangiogenesis factor in tumor progression. Nuclei are stained in blue (DAPI). Scale bars: 200 μm (A–C); 100 μm (D).

podoplanin plays an essential role in separating lymphatic vessels from blood vessels during mouse embryogenesis [28–30]. C-type lectin-like receptor 2 (CLEC-2), a functional podoplanin receptor, is abundantly expressed by platelets [31]. During embryogenesis, communication between blood circulation and primitive lymph sacs allows platelets to contact lymphatic endothelial cells expressing podoplanin. Subsequently, podoplanin/CLEC-2 interaction activates downstream signaling leading to blood coagulation. These clots are essential for separation of lymph sacs from blood vessels during mouse embryogenesis. Accordingly, podoplanin- or CLEC-2-null embryonic mice show defects in blood aggregation adjacent to primitive lymph sacs and exhibit altered lymphatic vessels filled with blood. Indeed, SLP-76 and Syk76, downstream effectors of the podoplanin/CLEC-2 axis, play a key role to separate lymphatic from blood vessels [32] (Fig. 4).

4. Lymphatic vessels connect the skin and lymph nodes in the immune system

The mammalian epidermis maintains a barrier to protect an organism from pathogens and immunogenic antigens. For this purpose, Langerhans cells are responsible for capturing hapten and then migrate to lymph nodes for antigen presentation. In fact, dendritic cells including Langerhans cells can enter the lymphatic vessels in the skin. Recent studies show that lymphatic endothelial cells in initial lymphatic vessels form a 'button-like junction', which represents a flap enabling dendritic cells to enter the lymphatic vessels without enzymatic digestion of the lymphatic endothelium [18,33].

Lymphatic vessels and lymph nodes cooperatively function as an immune system. Lymphatic vessels show a sinusoidal network pattern in lymph nodes. A recent study indicates that lymphatic endothelial cells and/or primitive lymph sacs are required for formation of the lymph node capsule in *Prox1* conditional null embryos [34]. Furthermore, these mice show altered positioning of hematopoietic cells within developing lymph nodes. In fact, lymph sacs are not required to initiate lymph node formation during mouse embryonic development; however, sinusoidal lymphatic endothelial cells are required for mesenchymal cell differentiation and attraction of lymphoid tissue inducer cells in developing mouse lymph nodes. Of interest, a recent study showed that CCL21, the chemokine responsible for attracting lymphoid tissue inducer cells, promotes formation of a new lymphoid-like reticular stromal network in B16-F10 melanoma-derived peri-tumoral stroma and recruitment of regulatory T-cells [35]. Such tumor cell-based manipulation of the host immune system leads to formation of a tolerogenic tumor microenvironment, facilitating tumor progression. In contrast, another recent study showed that a subset of lymphoid tissue-inducer cells that express the natural cytotoxicity receptor NKp46 contribute to antitumor immunity in B16 melanoma-associated tumor vasculature [36]. Importantly, NKp46-positive lymphoid tissue-inducer cells are activated by interleukin-12, and upregulate adhesion molecules in the tumor vasculature, resulting in recruitment of leukocytes and tumor suppression.

5. Pathological lymphangiogenesis requires diverse cell types

Florence Sabin, a twentieth century pioneer in anatomy, proposed in 1902 that lymphatic vessels arise from veins during mammalian embryogenesis [37]. This elegant concept was confirmed in 1999 by knockout of mouse *Prox1*. Null mice exhibited arrest of budding and sprouting of lymphatic endothelial cells from veins at E11.5–12.0, leading to absence of lymphatic

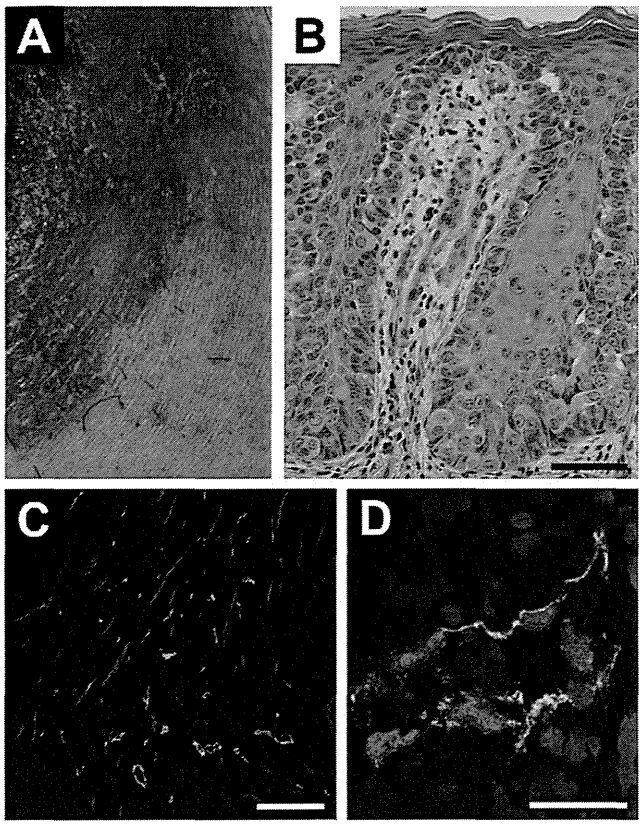

Fig. 3. Tumor lymphangiogenesis in extramammary Paget's disease (EMPD). (A) Macroscopic appearance of genitalia of a 68-year-old man with EMPD. A demarcated erythema was found with scale-crusts and small-sized erosions. (B) H&E stains show that Paget cells appear rounded in the hyperplastic epidermis and that dermal papillae are markedly elongated. Marked edema and penetration of capillary-sized blood vessels are observed within the papillary dermis, indicating that tumor-associated angiogenesis is induced in EMPD. (C) Double immunofluorescence for podoplanin (green) and von Willebrand factor, a blood vessel marker (red) show a marked increase in lymphatic and blood vessels within primary EMPD sites. (D) Podoplanin staining of tumor-associated lymphatic vessels (green) was also Prox1-positive (red), confirming their lymphatic identity. Nuclei are stained in blue (DAPI). Scale bars: 50 μm (B); 100 μm (C); 20 μm (D).

vasculature and embryonic lethality [9]. Thus, in embryonic mouse, physiological venous development is sufficient for lymphatic vascular development and other lymphatic precursors of hematopoietic or mesenchymal origin make marginal contribution to the process [38].

To gain insight into the significance of veins to lymphatic vascular development, a recent study showed that COUP-TFII, a key transcription factor functioning in specification of veins from arteries, plays an essential role to activate Prox1 expression during murine embryogenesis. COUP-TFII physically interacts with Prox1 to regulate lineage-specific genes in cultured lymphatic endothelial cells [39,40], Furthermore, the SRY-related HMG domain transcription factor Sox18 was shown to be an upstream regulator of Prox1 in venous lymphatic endothelial cell progenitors [41]. Thus, emerging evidence has shed light on molecular mechanisms underlying transcriptional regulation of lymphatic vessel development.

Although it resembles physiological lymphangiogenesis, pathological lymphangiogenesis following human renal transplantation employs additional lymphatic endothelial cells from bone marrow-derived precursors [42]. Trans-differentiating CD11b-positive macrophages also function in pathological lymphangiogenesis following penetrating keratoplasty in mouse cornea [43] or during cutaneous wound healing in a diabetic mouse model [44]. In addition, little or no incorporation of bone-marrow-derived endothelial progenitor cells was observed in experimental tumor models, indicating that pre-existing lymphatic vessels are largely required for tumor lymphangiogesis [45]. Activated macrophages are commonly acknowledged to be a major source of VEGF-C and/or VEGF-D, both of which potently induce new lymphatic vessel development during tumor progression. Tumor-associated macrophages were originally identified to promote tumor lymphangiogenesis in human uterine cervical cancers [46]. Later, several experimental or pathological studies indicate that tumor-associated macrophages contribute to new lymphatic vessel growth [47–49]. Of note, a mouse orthotopic xenograft model revealed that F4/80-positive macrophages are a major source of VEGF-C and VEGF-D, and that the cyclooxygenase-2 inhibitor etodolac reduces draining lymph node metastases in addition to tumor lymphangiogenesis [49]. Furthermore, mice harboring a mutation in the *csf-1* gene, which encodes macrophage colony-stimulating factor (M-CSF), demonstrated that M-CSF deficiency suppressed lymphangiogenesis and lymph node metastasis in experimental tumor models [50], supporting the concept that cells of the monocyte lineage play a fundamental role in promoting tumor-associated lymphangiogenesis.

6. Tumor lymphangiogenesis: inflammatory conditions enhance lymphatic vessel growth in a tumor microenvironment

Sentinel and/or regional lymph node metastasis are often the first indicators of spread of malignant tumors from the primary lesion. Furthermore, lymph node metastases in distant sites indicate disease progression in certain types of cancer. Therefore, the significance of lymph node metastasis is well documented in malignant neoplasms such as cutaneous melanoma [51]. Recent pathological studies show that tumor lymphangiogenesis promotes enhanced sentinel or regional lymph node metastasis in several types of malignant neoplasm, including cutaneous melanoma [52,53]. Importantly, tumor-associated lymphangiogenesis in melanoma patients is not only correlated with enhanced sentinel lymph node metastasis but also predicts reduced patient survival [47].

Vascular endothelial growth factor (VEGF)-C and its receptor VEGFR-3/Flt4 are essential for lymphatic vascular development (Fig. 5) [13,54]. Emerging evidence shows that VEGF-C/VEGFR-3 signaling also play a key role in tumor lymphangiogenesis [2,4,5]. VEGFR-3 blockade by neutralizing antibodies or a soluble form of VEGFR-3 markedly reduces VEGF-C-dependent tumor lymphangiogenesis and draining lymph node metastasis in experimental tumor models [55–57]. Based on this finding, a monoclonal single chain fragment targeting human VEGF-C was recently generated using phase display techniques [58]. This small fragment inhibits binding of VEGF-C not only to VEGFR-3/Flt4 but also to VEGFR-2/KDR. Intriguingly, recent studies indicate that VEGFR-2 is an endogenous inhibitor of lymphangiogenesis [59,60]. *VEGFR-2/KDR* yields two splicing variant forms with or without the transmembrane and intracellular tyrosine kinase domains. In fact, avascular areas such as mouse epidermis or cornea abundantly express the soluble form of VEGFR (sVEGFR)-2/KDR, which binds to VEGF-C, demonstrating that sVEGFR-2 is an endogenous VEGF-C antagonist *in vivo* [59]. Meanwhile, membrane-bound VEGFR-2 has been shown to internalize VEGF-C by inducing formation of a VEGFR-2/VEGF-C complex in blood vascular endothelial cells, leading to delayed lymphangiogenesis in a mouse corneal micropocket assay [60]. However, it should be noted that lymphatic endothelial cells express VEGFR-2, which responds to VEGF-A *in vitro* and *in vivo* (Fig. 5) [14,61–63].

In addition to VEGF-C, pathological lymphangiogenesis is induced by pro-inflammatory cytokines. As noted, physiological

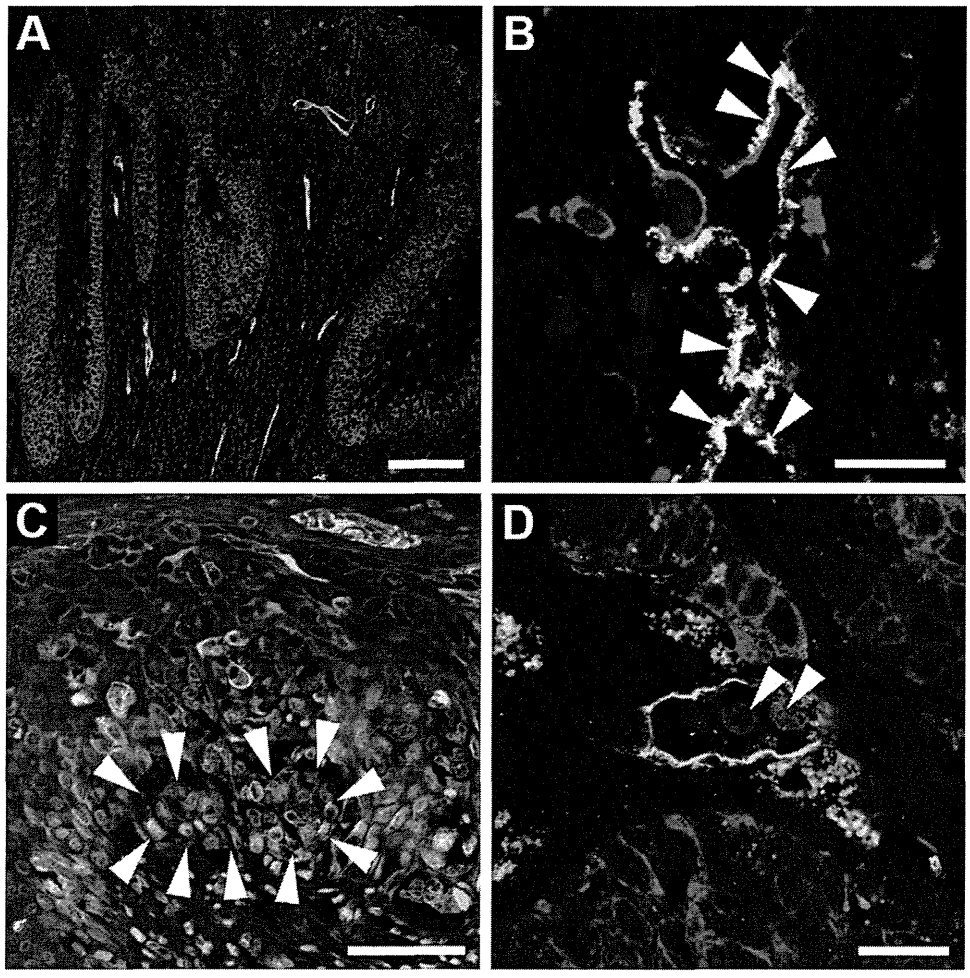

Fig. 4. Phenotypic alterations in invasive Paget cells and tumor-associated lymphatic vessels in EMPD. (A) Double immunofluorescence for cytokeratin 7 (red) and podoplanin (green) in carcinoma *in situ*. Respective stains are mutually exclusive, indicating no association between Paget cells and tumor-associated lymphatic vessels. (B) Double immunofluorescence for CXCL12 (red) and LYVE-1 (green) in carcinoma *in situ*. Tumor associated-lymphatic endothelial cells express CXCL12 (arrowheads, yellow), a chemoattractant for invasive tumor cells. (C) Double immunofluorescence for E-cadherin (green) and N-cadherin (red) in invasive EMPD. Little or no E-cadherin was observed in invasive Paget cells, whereas these tumor cells express N-cadherin, a mesenchymal marker in dermo-epidermal junction (arrowheads), indicating that invasive Paget cells undergo epithelial-to-mesenchymal transitions. Nuclei are stained in blue (DAPI). (D) Double immunofluorescence for cytokeratin 7 (red) and podoplanin (green) in invasive EMPD. Among massive invasion by Paget cells within the stroma, podoplanin-positive lymphatic vessels are enlarged and invaded by Paget cells (arrowheads). Nuclei are stained in blue (DAPI). Scale bars: 100 μm (A); 50 μm (B and C); 30 μm (D).

lymphatic vessel development is regulated by transcription factors such as Prox1 and by the growth factor VEGF-C. Furthermore, several growth factors and cytokines have been shown to induce experimental and/or pathological lymphangiogenesis in animal models. Recent studies show that tumor necrosis factor-α and interleukin-1β play a critical role in bacteria-induced airway inflammation [64,65]. Furthermore, transgenic overexpression of hepatocyte growth factor induces marked density and enlargement of lymphatic vessels in the skin [66]. Meanwhile, functional blokade of transforming growth factor (TGF)-β leads to marked increases in new lymphatic vessel growth in the inflammatory tissue response or in experimental mouse tumor models, indicating that TGF-β negatively regulates pathological lymphangiogenesis [67]. In mouse, targeted VEGF-A overexpression in skin promotes lymphangiogenesis within primary tumor sites in a chemically-induced mouse skin carcinogenesis regimen (Fig. 3), leading to enhanced draining lymph node metastasis [14]. Indeed, epidermal overexpression of VEGF-A promotes significant enlargement of lymphatic vessels in cutaneous delayed-type hypersensitivity reactions [68], UVB irradiation [69] or cutaneous wound healing [63]. Accordingly, adenoviral expression of VEGF-A in mouse skin also promotes lymphangiogenesis as well as angiogenesis [62], supporting the idea that pathological lymphangiogenesis is mediated by pro-inflammatory cytokines and/or growth factors such as VEGF-A. Importantly, the inflammatory tissue response likely promotes enhanced tumor-associated lymphangiogenesis. Indeed, marked lymphangiogenesis has been observed in cutaneous malignant melanoma [52], extramammary Paget's disease [16], inflammatory breast cancer [70], and in an experimental ovarian cancer model [48] in which an inflammatory condition is likely induced.

7. Molecular profiles of lymphatic endothelium in pathological conditions

Tumor-associated lymphatic vessels are different from normal lymphatic vessels in the skin. Recent studies show that tumor-associated lymphatic endothelial cells show molecular profiles distinct from normal lymphatic endothelium [71]. Tumor-associated lymphatic endothelial cells were originally isolated from an experimental tumor model bearing T241 fibrosarcoma cells overexpressing VEGF-C. Comparative gene profiles showed that the endothelial specific adhesion molecule (ESAM), the transforming growth factor-β co-receptor endoglin, and CD200 are up-regulated, whereas the extracellular matrix molecule biglycan is down-regulated in cultured tumor-associated lymphatic endothe-

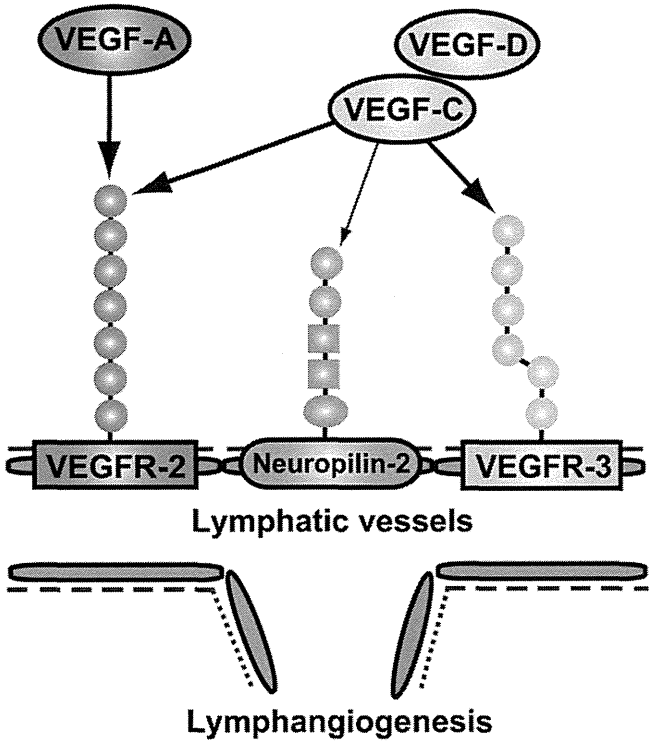

Fig. 5. VEGF family members and their cognate receptor tyrosine kinases in the tumor micoenvironment. VEGF-C and VEGF-D, potent VEGFR-3 ligands, promote lymphangiogenesis. Neuropilin-2, the VEGF-C co-receptor, is induced in lymphatic endothelial cells during tumor progression. Pro-inflammatory cytokines such as VEGF-A also promote pathological lymphangiogenesis.

lial cells relative to dermal lymphatic endothelial cells. Accordingly, ESAM was found specifically expressed in tumor-associated lymphatic vessels in VEGF-C-expressing T241 tumors and in human cancers such as head and neck squamous carcinomas (HNSCC). Importantly, a striking correlation was observed between the incidence of ESAM-positive, tumor-associated lymphatic vessels and the presence of lymph node metastases in patients with HNSCC, indicating that ESAM may have a prognostic value in relation to tumor lymphangiogesis [71].

Neuropilin-2, the VEGF-C co-receptor, is expressed in lymphatic vessels during mouse embryonic development [72]. Recent studies in either experimental tumor models [73] or human skin cancers [16] show that neuropilin-2 is expressed in tumor-associated lymphatic vessels. Importantly, functional blockade of neuropilin-2 using a neutralizing antibody decreased tumor lymphangiogenesis and induced significant delay of sentinel lymph node metastasis in experimental tumor models, indicating that neuropilin-2 may be an alternative target to prevent lymph node metastasis through lymphatic vessels [73].

Cutaneous lymphatic vessels attract immune cells such as leukocytes or dendritic cells to promote immune surveillance and the inflammatory tissue response. LECs, but not normal blood vascular endothelial cells, are a major source of CCL21, a functional ligand and chemokine for CCR7, while dendritic cells and T leukocytes express the CCR7 receptor [74,75]. Importantly, VEGF-C or the pro-inflammatory cytokine TNF-α increases CCL21 secretion in cultured lymphatic endothelial cells, leading to enhanced transmigration of either mature dendritic cells or CCR7-positive tumor cells towards lymphatic endothelial cells *in vitro* [76,77]. In fact, the CCR7/CCL21 axis reportedly promotes lymph node metastasis in malignant neoplasms such as breast cancer or malignant melanoma [78–80]. Furthermore, another chemokine network, the CXCR4/CXCL12 axis, has been demonstrated to promote lymphatic trafficking of dendritic cells in inflamed mouse skin, indicating that lymphatic vessels likely engage CXCR4-positive dendritic cells by producing CXCL12 [81]. In several types of cancer, metastatic tumor cells reportedly express CXCR4, leading to increased incidence of sentinel and/or regional lymph node metastasis [78,82]. In fact, tumor-associated rather than normal lymphatic vessels express CXCL12 during tumor progression (Fig. 4B) [16]. Thus, lymphatic vessels in pathologic conditions employ physiological mechanisms to attract immune cells.

Invasion is a biological process that promotes tumor growth and survival within primary sites. Recent studies show that tumor cells of epithelial origin may switch to a mesenchymal phenotype promoting stromal invasion (Fig. 4C). A pathological epithelial-to-mesenchymal transition (EMT) is induced by transcription factors such as Snail. Our recent study showed that A431 cells increase their CXCR4 expression following ectopic expression of Snail. Importantly, CXCR4 levels are further enhanced by TGF-β1, another key regulator of EMT, indicating that EMT may significantly increase CXCR4 expression during tumor cell invasion of stroma or tumor-associated vasculature (Fig. 4D). Thus, multiple chemokine signals likely mediate tumor cell invasion of lymphatic vessels in the tumor microenvironment and further dissemination in the lymph nodes

8. Lymph node lymphangiogenesis that facilitates metastases during tumor progression

Experimental tumor models analyzed by us and others indicate that draining lymph nodes induce a new sinusoidal lymphatic network prior to tumor metastasis [14,15,83,84]. This nodal lymphangiogenesis likely contributes to enhanced distant lymph node and/or distant organ metastases. Importantly, lymph node lymphangiogenesis is induced in certain human cancers, such as extramammary Paget's disease (EMPD) (Fig. 6A and B) [16]. Our recent study of 116 patients, the largest EMPD cohort analyzed, revealed markedly increased lymph node lymphangiogenesis during lymph node metastasis, and that event was significantly correlated with progression of nodal metastasis. Furthermore, tumor cell invasion of the sinusoidal lymphatic network indicates the presence of distant lymph node and/or distant organ metastasis, leading to reduced patient survival. In fact, marked progression of nodal lymphangiogenesis may be seen as multiple lymphadenopathy in EMPD, indicating clinical relevance [17]. Most importantly, new lymphatic vessel growth is likely induced in draining lymph nodes, even before tumors metastasize in EMPD (Fig. 6A). Thus, the functional role of the 'lymphvascular niche' needs to be clarified in order to understand how the newly formed lymphatic network contributes to tumor spread via lymphatic vessels [27]. Notably, recent studies using experimental mouse models also show that nodal lymphangiogenesis is induced in cutaneous inflammatory tissue response [85–87]. Lymph node lymphangiogenesis likely contributes to increased migration of cutaneous dendritic cells to draining lymph nodes, maintenance of lymphatic flow, and resolution of inflammation.

9. Perspectives

Recent advances in molecular technologies have enabled researchers and clinicians to visualize lymphatic vessels using specific antibodies. However, a fundamental question remains as to whether lymphatic vessels play a functional role in the pathogenesis of cutaneous diseases. In 1627 the anatomist and surgeon Gasparo Aselli discovered physiological flow in lymphatic vessels using vivisection of the mesentery in dogs [88]. His observations revealed that one function of lymphatic vessels was to transport nutrients from the intestine to proximal organs. His

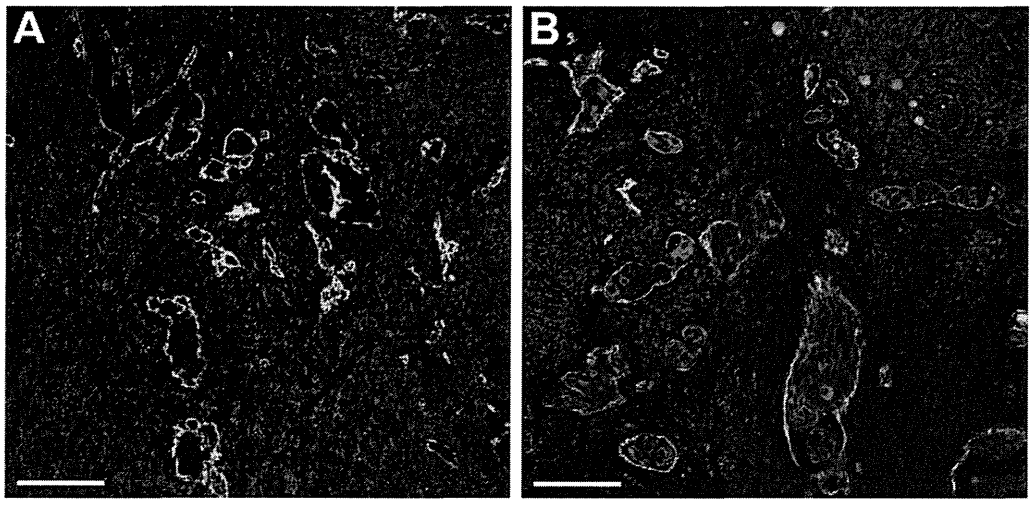

Fig. 6. Lymph node lymphangiogenesis in EMPD. Double immunofluorescence stains for von Willebrand factor (red) and podoplanin (green) in regional lymph nodes prior to tumor metastasis. New lymphatic vessel growth was observed prior to tumor cell metastasis, indicating induction of a "lymphvascular niche" for metastatic Paget cells. H&E staining shows no metastatic foci in serial sections. (B) Double immunofluorescence for cytokeratin 7 (red) and podoplanin (green) in metastatic lymph nodes. Note that metastatic Paget cells invade the tumor-associated sinusoidal lymphatic network. Nuclei are stained in blue (DAPI). Scale bars: 200 μm (A and B).

visualization of invisible vessels using white-colored lymph was a historic scientific achievement. Today, it is necessary to re-visualize the lymphatic flow to identify a functional role of lymphatic vessels in pathologic conditions such as the immune response [89] or cancer progression [90]. This experimental approach will provide a fundamental understanding of mechanisms and pathogenesis of diseases associated with lymphatic vessels. Another important question is whether lymphatic vessels could be a therapeutic target to slow disease progression. Recently, lymphatic vessel alteration was shown to be a major cause of UVB or bacterial pathogen-induced acute skin inflammation [87,91] and chronic inflammation in K14-VEGF-A transgenic mice [92]. Importantly, VEGF-C-induced VEGFR-3 activation induced marked reduction of the inflammatory tissue response to baseline levels in those experimental models [87,91,92], indicating that lymphatic vessels can be targeted to control inflammatory human skin diseases, including psoriasis vulgaris.

Pathological lymphangiogenesis is a stepwise process requiring proliferation and migration of lymphatic endothelial cells. However, it remains unclear whether lymphatic vessels initially undergo vascular hyperpermeability, potentially induced by altered cell–cell contact. Furthermore, it remains unclear whether enzymatic digestion of basement membranes occurs in lymphatic vessels during neovascularization. Therefore, mechanisms underlying pathological lymphangiogenesis must be clarified to better understand lymphatic vessel alterations that may underlie the pathogenesis of cutaneous diseases.

Acknowledgments

The author thanks Dr. Michael Detmar for images of the chemically-induced mouse skin carcinogenesis study. This work was supported by a Grant-in-Aid for Scientific Research on Priority Areas (MEXT20013032).

References

[1] Alitalo K, Tammela T, Petrova TV. Lymphangiogenesis in development and human disease. Nature 2005;438(15):946–53.
[2] Skobe M, Hawighorst T, Jackson DG, Prevo R, Janes L, Velasco P, et al. Induction of tumor lymphangiogenesis by VEGF-C promotes breast cancer metastasis. Nature Medicine 2001;7(2):192–8.
[3] Stacker SA, Caesar C, Baldwin ME, Thornton GE, Williams RA, Prevo R, et al. VEGF-D promotes the metastatic spread of tumor cells via the lymphatics. Nature Medicine 2001;7(2):186–91.
[4] Mandriota SJ, Jussila L, Jeltsch M, Compagni A, Baetens D, Prevo R, et al. Vascular endothelial growth factor-C-mediated lymphangiogenesis promotes tumour metastasis. The EMBO Journal 2001;20(4):672–82.
[5] Karpanen T, Egeblad M, Karkkainen MJ, Kubo H, Yla-Herttuala S, Jaattela M, et al. Vascular endothelial growth factor C promotes tumor lymphangiogenesis and intralymphatic tumor growth. Cancer Research 2001;61(5):1786–90.
[6] Oliver G, Detmar M. The rediscovery of the lymphatic system. Old and new insights into the development and biological function of lymphatic vascular system. Genes & Development 2002;16(7):773–83.
[7] Tammela T, Alitalo K. Lymphangiogenesis: molecular mechanisms and future promise. Cell 2010;140(4):460–76.
[8] Wang Y, Oliver G. Current views on the function of the lymphatic vasculature in health and disease. Genes & Development 2010;24(19):2115–26.
[9] Wigle JT, Oliver G. Prox1 function is required for the development of the murine lymphatic system. Cell 1999;98(6):769–78.
[10] Oliver G, Sosa-Pineda B, Geisendorf S, Spana EP, Doe CQ, Gruss P. Prox 1, a prospero-related homeobox gene expressed during mouse development. Mechanisms of Development 1993;44:3–16.
[11] Pajusola K, Aprelikova O, Korhonen J, Kaipainen A, Pertovaara L, Alitalo R, et al. FLT4 receptor tyrosine kinase contains seven immunoglobulin-like loops and is expressed in multiple human tissues and cell lines. Cancer Research 1992;52(20):5738–43.
[12] Joukov V, Pajusola K, Kaipainen A, Chilov D, Lahtinen I, Kukk E, et al. A novel vascular endothelial growth factor, VEGF-C, is a ligand for the Flt4 (VEGFR-3) and KDR (VEGFR-2) receptor tyrosine kinases. The EMBO Journal 1996;15(7):1751.
[13] Karkkainen MJ, Haiko P, Sainio K, Partanen J, Taipale J, Petrova TV, et al. Vascular endothelial growth factor C is required for sprouting of the first lymphatic vessels from embryonic veins. Nature Immunology 2004;5(1):74–80.
[14] Hirakawa S, Kodama S, Kunstfeld R, Kajiya K, Brown LF, Detmar M. VEGF-A induces tumor and sentinel lymph node lymphangiogenesis and promotes lymphatic metastasis. The Journal of Experimental Medicine 2005;201(7):1089–99.
[15] Hirakawa S, Brown LF, Kodama S, Paavonen K, Alitalo K, Detmar M. VEGF-C-induced lymphangiogenesis in sentinel lymph nodes promotes tumor metastasis to distant sites. Blood 2007;109(3):1010–7.
[16] Hirakawa S, Detmar M, Kerjaschki D, Nagamatsu S, Matsuo K, Tanemura A, et al. Nodal lymphangiogenesis and metastasis: Role of tumor-induced lymphatic vessel activation in extramammary Paget's disease. The American Journal of Pathology 2009;175(5):2235–48.
[17] Hirakawa S, Tanemura A, Mori H, Katayama I, Hashimoto K. Multiple lymphadenopathy as an initial sign of extramammary Paget's disease. The British Journal of Dermatology; in press.
[18] Baluk P, Fuxe J, Hashizume H, Romano T, Lashnits E, Butz S, et al. Functionally specialized junctions between endothelial cells of lymphatic vessels. The Journal of Experimental Medicine 2007;204(10):2349–62.
[19] Harvey NL, Srinivasan RS, Dillard ME, Johnson NC, Witte MH, Boyd K, et al. Lymphatic vascular defects promoted by Prox1 haploinsufficiency cause adult-onset obesity. Nature Genetics 2005;37(10):1072–81.
[20] Machnik A, Neuhofer W, Jantsch J, Dahlmann A, Tammela T, Machura K, et al. Macrophages regulate salt-dependent volume and blood pressure by a vascular endothelial growth factor-C-dependent buffering mechanism. Nature Medicine 2009;15(5):545–52.
[21] Lim HY, Rutkowski JM, Helft J, Reddy ST, Swartz MA, Randolph GJ, et al. Hypercholesterolemic mice exhibit lymphatic vessel dysfunction and degeneration. The American Journal of Pathology 2009;175(3):1328–37.

[22] Banerji S, Ni J, Wang SX, Clasper S, Su J, Tammi R, et al. LYVE-1, a new homologue of the CD44 glycoprotein, is a lymph-specific receptor for hyaluronan. The Journal of Cell Biology 1999;144(4):789–801.
[23] Gale NW, Prevo R, Espinosa J, Ferguson DJ, Dominguez MG, Yancopoulos GD, et al. Normal lymphatic development and function in mice deficient for the lymphatic hyaluronan receptor LYVE-1. Molecular and Cellular Biology 2007;27(2):595–604.
[24] Luong MX, Tam J, Lin Q, Hagendoorn J, Moore KJ, Padera TP, et al. Lack of lymphatic vessel phenotype in LYVE-1/CD44 double knockout mice. Journal of Cellular Physiology 2009;219(2):430–7.
[25] Huang SS, Liu IH, Smith T, Shah MR, Johnson FE, Huang JS. CRSBP-1/LYVE-1-null mice exhibit identifiable morphological and functional alterations of lymphatic capillary vessels. FEBS Letters 2006;580(26):6259–68.
[26] Breiteneder-Geleff S, Matsui K, Soleiman A, Meraner P, Poczewski H, Kalt R, et al. Podoplanin, novel 43-kd membrane protein of glomerular epithelial cells, is down-regulated in puromycin nephrosis. The American Journal of Pathology 1997;151(4):1141–52.
[27] Hirakawa S. From tumor lymphangiogenesis to lymphvascular niche. Cancer Science 2009;100(6):983–9.
[28] Uhrin P, Zaujec J, Breuss JM, Olcaydu D, Chrenek P, Stockinger H, et al. Novel function for blood platelets and podoplanin in developmental separation of blood and lymphatic circulation. Blood 2010;115(19):3997–4005.
[29] Bertozzi CC, Schmaier AA, Mericko P, Hess 2F P.R., Zou Z, Chen M, et al. Platelets regulate lymphatic vascular development through CLEC-2-SLP-76 signaling. Blood 2010;116(4):661–70.
[30] Suzuki-Inoue K, Inoue O, Ding G, Nishimura S, Hokamura K, Eto K, et al. Essential in vivo roles of the C-type lectin receptor CLEC-2: embryonic/neonatal lethality of CLEC-2-deficient mice by blood/lymphatic misconnections and impaired thrombus formation of CLEC-2-deficient platelets. The Journal of Biological Chemistry 2010;285(32):24494–507.
[31] Suzuki-Inoue K, Kato Y, Inoue O, Kaneko MK, Mishima K, Yatomi Y, et al. Involvement of the snake toxin receptor CLEC-2, in podoplanin-mediated platelet activation, by cancer cells. The Journal of Biological Chemistry 2007;282(36):25993–6001.
[32] Abtahian F, Guerriero A, Sebzda E, Lu MM, Zhou R, Mocsai A, et al. Regulation of blood and lymphatic vascular separation by signaling proteins SLP-76 and Syk. Science (New York NY) 2003;299(5604):247–51.
[33] Pflicke H, Sixt M. Preformed portals facilitate dendritic cell entry into afferent lymphatic vessels. The Journal of Experimental Medicine 2009;206(13):2925–35.
[34] Vondenhoff MF, van de Pavert SA, Dillard ME, Greuter M, Goverse G, Oliver G, et al. Lymph sacs are not required for the initiation of lymph node formation. Development (Cambridge England) 2009;136(1):29–34.
[35] Shields JD, Kourtis IC, Tomei AA, Roberts JM, Swartz MA. Induction of lymphoidlike stroma and immune escape by tumors that express the chemokine CCL21. Science (New York NY) 2010;328(5979):749–52.
[36] Eisenring M, vom Berg J, Kristiansen G, Saller E, Becher B. IL-12 initiates tumor rejection via lymphoid tissue-inducer cells bearing the natural cytotoxicity receptor NKp46. Nature Immunology 2010;11(11):1030–8.
[37] Sabin FR. On the origin of the lymphatic system from the veins and the development of the lymph hearts and thoracic duct in the pig. American Journal of Anatomy 1902;1:367–91.
[38] Srinivasan RS, Dillard ME, Lagutin OV, Lin FJ, Tsai S, Tsai MJ, et al. Lineage tracing demonstrates the venous origin of the mammalian lymphatic vasculature. Genes & Development 2007;21(19):2422–32.
[39] Lee S, Kang J, Yoo J, Ganesan SK, Cook SC, Aguilar B, et al. Prox1 physically and functionally interacts with COUP-TFII to specify lymphatic endothelial cell fate. Blood 2009;113(8):1856–9.
[40] Yamazaki T, Yoshimatsu Y, Morishita Y, Miyazono K, Watabe T. COUP-TFII regulates the functions of Prox1 in lymphatic endothelial cells through direct interaction. Genes Cells 2009;14(3):425–34.
[41] Francois M, Caprini A, Hosking B, Orsenigo F, Wilhelm D, Browne C, et al. Sox18 induces development of the lymphatic vasculature in mice. Nature 2008;456(7222):643–7.
[42] Kerjaschki D, Huttary N, Raab I, Regele H, Bojarski-Nagy K, Bartel G, et al. Lymphatic endothelial progenitor cells contribute to de novo lymphangiogenesis in human renal transplants. Nature Medicine 2006;12(2):230–4.
[43] Maruyama K, Ii M, Cursiefen C, Jackson DG, Keino H, Tomita M, et al. Inflammation-induced lymphangiogenesis in the cornea arises from CD11b-positive macrophages. The Journal of Clinical Investigation 2005;115(9):2363–72.
[44] Maruyama K, Asai J, Ii M, Thorne T, Losordo DW, D'Amore PA. Decreased macrophage number and activation lead to reduced lymphatic vessel formation and contribute to impaired diabetic wound healing. The American Journal of Pathology 2007;170(4):1178–91.
[45] He Y, Rajantie I, Ilmonen M, Makinen T, Karkkainen MJ, Haiko P, et al. Preexisting lymphatic endothelium but not endothelial progenitor cells are essential for tumor lymphangiogenesis and lymphatic metastasis. Cancer Research 2004 Jun 1;64(11):3737–40.
[46] Schoppmann SF, Birner P, Stockl J, Kalt R, Ullrich R, Caucig C, et al. Tumor-associated macrophages express lymphatic endothelial growth factors and are related to peritumoral lymphangiogenesis. The American Journal of Pathology 2002;161(3):947–56.
[47] Dadras SS, Lange-Asschenfeldt B, Velasco P, Nguyen L, Vora A, Muzikansky A, et al. Tumor lymphangiogenesis predicts melanoma metastasis to sentinel lymph nodes. Modern Pathology 2005;18(9):1232–42.
[48] Jeon BH, Jang C, Han J, Kataru RP, Piao L, Jung K, et al. Profound but dysfunctional lymphangiogenesis via vascular endothelial growth factor ligands from CD11b+ macrophages in advanced ovarian cancer. Cancer Research 2008;68(4):1100–9.
[49] Iwata C, Kano MR, Komuro A, Oka M, Kiyono K, Johansson E, et al. Inhibition of cyclooxygenase-2 suppresses lymph node metastasis via reduction of lymphangiogenesis. Cancer Research 2007;67(21):10181–9.
[50] Kubota Y, Takubo K, Shimizu T, Ohno H, Kishi K, Shibuya M, et al. M-CSF inhibition selectively targets pathological angiogenesis and lymphangiogenesis. The Journal of Experimental Medicine 2009;206(5):1089–102.
[51] Balch CM, Gershenwald JE, Soong SJ, Thompson JF, Atkins MB, Byrd DR, et al. Final version of 2009 AJCC melanoma staging and classification. Journal of Clinical Oncology 2009;27(36):6199–206.
[52] Dadras SS, Paul T, Bertoncini J, Brown LF, Muzikansky A, Jackson DG, et al. Tumor lymphangiogenesis: a novel prognostic indicator for cutaneous melanoma metastasis and survival. The American Journal of Pathology 2003;162(6):1951–60.
[53] Van der Auwera I, Cao Y, Tille JC, Pepper MS, Jackson DG, Fox SB, et al. First international consensus on the methodology of lymphangiogenesis quantification in solid human tumours. British Journal of Cancer 2006;95(12):1611–25.
[54] Makinen T, Jussila L, Veikkola T, Karpanen T, Kettunen MI, Pulkkanen KJ, et al. Inhibition of lymphangiogenesis with resulting lymphedema in transgenic mice expressing soluble VEGF receptor-3. Nature Medicine 2001;7(2):199–205.
[55] He Y, Kozaki K, Karpanen T, Koshikawa K, Yla-Herttuala S, Takahashi T, et al. Suppression of tumor lymphangiogenesis and lymph node metastasis by blocking vascular endothelial growth factor receptor 3 signaling. Journal of the National Cancer Institute 2002;94(11):819–25.
[56] Shimizu K, Kubo H, Yamaguchi K, Kawashima K, Ueda Y, Matsuo K, et al. Suppression of VEGFR-3 signaling inhibits lymph node metastasis in gastric cancer. Cancer Science 2004;95(4):328–33.
[57] Roberts N, Kloos B, Cassella M, Podgrabinska S, Persaud K, Wu Y, et al. Inhibition of VEGFR-3 activation with the antagonistic antibody more potently suppresses lymph node and distant metastases than inactivation of VEGFR-2. Cancer Research 2006;66(5):2650–7.
[58] Rinderknecht M, Villa A, Ballmer-Hofer K, Neri D, Detmar M. Phage-derived fully human monoclonal antibody fragments to human vascular endothelial growth factor-C block its interaction with VEGF receptor-2 and 3. PloS one 2010;5(8):e11941.
[59] Albuquerque RJ, Hayashi T, Cho WG, Kleinman ME, Dridi S, Takeda A, et al. Alternatively spliced vascular endothelial growth factor receptor-2 is an essential endogenous inhibitor of lymphatic vessel growth. Nature Medicine 2009;15(9):1023–30.
[60] Nakao S, Zandi S, Hata Y, Kawahara S, Arita R, Schering A, et al. Blood vessel endothelial VEGFR-2 delays lymphangiogenesis: an endogenous trapping mechanism links lymph- and angiogenesis. Blood; in press.
[61] Hirakawa S, Hong YK, Harvey N, Schacht V, Matsuda K, Libermann T, et al. Identification of vascular lineage-specific genes by transcriptional profiling of isolated blood vascular and lymphatic endothelial cells. The American Journal of Pathology 2003;162(2):575–86.
[62] Nagy JA, Vasile E, Feng D, Sundberg C, Brown LF, Detmar MJ, et al. Vascular permeability factor/vascular endothelial growth factor induces lymphangiogenesis as well as angiogenesis. The Journal of Experimental Medicine 2002;196(11):1497–506.
[63] Hong YK, Lange-Asschenfeldt B, Velasco P, Hirakawa S, Kunstfeld R, Brown LF, et al. VEGF-A promotes tissue repair-associated lymphatic vessel formation via VEGFR-2 and the alpha1beta1 and alpha2beta1 integrins. FASEB Journal 2004;18(10):1111–3.
[64] Baluk P, Yao LC, Feng J, Romano T, Jung SS, Schreiter JL, et al. TNF-alpha drives remodeling of blood vessels and lymphatics in sustained airway inflammation in mice. The Journal of Clinical Investigation 2009;119(10):2954–64.
[65] Yao LC, Baluk P, Feng J, McDonald DM. Steroid-resistant lymphatic remodeling in chronically inflamed mouse airways. The American Journal of Pathology 2010;176(3):1525–41.
[66] Kajiya K, Hirakawa S, Ma B, Drinnenberg I, Detmar M. Hepatocyte growth factor promotes lymphatic vessel formation and function. The EMBO Journal 2005;24(16):2885–95.
[67] Oka M, Iwata C, Suzuki HI, Kiyono K, Morishita Y, Watabe T, et al. Inhibition of endogenous TGF-beta signaling enhances lymphangiogenesis. Blood 2008;111(9):4571–9.
[68] Kunstfeld R, Hirakawa S, Hong YK, Schacht V, Lange-Asschenfeldt B, Velasco P, et al. VEGF-A plays a key role in the induction of chronic inflammation and the associated lymphangiogenic response. Blood 2004;104(4):1048–57.
[69] Kajiya K, Hirakawa S, Detmar M. Vascular endothelial growth factor-A mediates ultraviolet B-induced impairment of lymphatic vessel function. The American Journal of Pathology 2006;169(4):1496–503.
[70] Van den Eynden GG, Vandenberghe MK, van Dam PJ, Colpaert CG, van Dam P, Dirix LY, et al. Increased sentinel lymph node lymphangiogenesis is associated with nonsentinel axillary lymph node involvement in breast cancer patients with a positive sentinel node. Clinical Cancer Research 2007;13(18 Pt 1):5391–7.
[71] Clasper S, Royston D, Baban D, Cao Y, Ewers S, Butz S, et al. A novel gene expression profile in lymphatics associated with tumor growth and nodal metastasis. Cancer Research 2008;68(18):7293–303.

[72] Yuan L, Moyon D, Pardanaud L, Breant C, Karkkainen MJ, Alitalo K, et al. Abnormal lymphatic vessel development in neuropilin 2 mutant mice. Development (Cambridge England) 2002;129(20):4797–806.
[73] Caunt M, Mak J, Liang WC, Stawicki S, Pan Q, Tong RK, et al. Blocking neuropilin-2 function inhibits tumor cell metastasis. Cancer Cell 2008;13(4):331–42.
[74] Alvarez D, Vollmann EH, von Andrian UH. Mechanisms and consequences of dendritic cell migration. Immunity 2008;29(3):325–42.
[75] Debes GF, Arnold CN, Young AJ, Krautwald S, Lipp M, Hay JB, et al. Chemokine receptor CCR7 required for T lymphocyte exit from peripheral tissues. Nature Immunology 2005;6(9):889–94.
[76] Johnson LA, Jackson DG. Inflammation-induced secretion of CCL21 in lymphatic endothelium is a key regulator of integrin-mediated dendritic cell transmigration. International Immunology 2010;22(10):839–49.
[77] Issa A, Le TX, Shoushtari AN, Shields JD, Swartz MA. Vascular endothelial growth factor-C and C-C chemokine receptor 7 in tumor cell-lymphatic cross-talk promote invasive phenotype. Cancer Research 2009;69(1):349–57.
[78] Muller A, Homey B, Soto H, Ge N, Catron D, Buchanan ME, et al. Involvement of chemokine receptors in breast cancer metastasis. Nature 2001;410(6824):50–6.
[79] Takeuchi H, Fujimoto A, Tanaka M, Yamano T, Hsueh E, Hoon DS. CCL21 chemokine regulates chemokine receptor CCR7 bearing malignant melanoma cells. Clinical Cancer Research 2004;10(7):2351–8.
[80] Wiley HE, Gonzalez EB, Maki W, Wu MM, Hwang ST. Expression of CC chemokine receptor-7 and regional lymph node metastasis of B16 murine melanoma. Journal of the National Cancer Institute 2001;93(21):1638–43.
[81] Kabashima K, Shiraishi N, Sugita K, Mori T, Onoue A, Kobayashi M, et al. CXCL12–CXCR4 engagement is required for migration of cutaneous dendritic cells. The American Journal of Pathology 2007;171(4):1249–57.
[82] Kucia M, Reca R, Miekus K, Wanzeck J, Wojakowski W, Janowska-Wieczorek A, et al. Trafficking of normal stem cells and metastasis of cancer stem cells involve similar mechanisms: pivotal role of the SDF-1-CXCR4 axis. Stem cells (Dayton Ohio) 2005;23(7):879–94.
[83] Harrell MI, Iritani BM, Ruddell A. Tumor-induced sentinel lymph node lymphangiogenesis and increased lymph flow precede melanoma metastasis. The American Journal of Pathology 2007;170(2):774–86.
[84] Qian CN, Berghuis B, Tsarfaty G, Bruch M, Kort EJ, Ditlev J, et al. Preparing the "soil": the primary tumor induces vasculature reorganization in the sentinel lymph node before the arrival of metastatic cancer cells. Cancer Research 2006;66(21):10365–76.
[85] Angeli V, Ginhoux F, Llodra J, Quemeneur L, Frenette PS, Skobe M, et al. B cell-driven lymphangiogenesis in inflamed lymph nodes enhances dendritic cell mobilization. Immunity 2006;(February):203–15.
[86] Halin C, Tobler NE, Vigl B, Brown LF, Detmar M. VEGF-A produced by chronically inflamed tissue induces lymphangiogenesis in draining lymph nodes. Blood 2007;110(9):3158–67.
[87] Kataru RP, Jung K, Jang C, Yang H, Schwendener RA, Baik JE, et al. Critical role of CD11b+ macrophages and VEGF in inflammatory lymphangiogenesis, antigen clearance, and inflammation resolution. Blood 2009;113(22):5650–9.
[88] Asellius G. De lactibus sive lacteis venis, quarto vasorum mesarai corum genere nova invento. Milan: Mediolani; 1627.
[89] Reddy ST, van der Vlies AJ, Simeoni E, Angeli V, Randolph GJ, O'Neil CP, et al. Exploiting lymphatic transport and complement activation in nanoparticle vaccines. Nature Biotechnology 2007;25(10):1159–64.
[90] Proulx ST, Luciani P, Derzsi S, Rinderknecht M, Mumprecht V, Leroux JC, et al. Quantitative imaging of lymphatic function with liposomal indocyanine green. Cancer Research 2010;70(18):7053–62.
[91] Kajiya K, Sawane M, Huggenberger R, Detmar M. Activation of the VEGFR-3 pathway by VEGF-C attenuates UVB-induced edema formation and skin inflammation by promoting lymphangiogenesis. Journal of Investigative Dermatology 2009;129(5):1292–8.
[92] Huggenberger R, Ullmann S, Proulx ST, Pytowski B, Alitalo K, Detmar M. Stimulation of lymphangiogenesis via VEGFR-3 inhibits chronic skin inflammation. The Journal of Experimental Medicine 2010;207(10):2255–69.

Satoshi Hirakawa, M.D., Ph.D. is Assistant Professor at Department of Dermatology in Ehime University Graduate School of Medicine, Japan. He received his M.D. degree in 1996 and Ph.D. degree in 2001 from Okayama University Medical School, Japan. From 2001 to 2005, he served as a postdoctoral fellow at Cutaneous Biology Research Center, Massachusetts General Hospital and Harvard Medical School, U.S.A. under the supervision by Prof. Dr. Michael Detmar. Since 2009, he is a faculty at Department of Cell Growth and Tumor Regulation in Ehime Proteo-Medicine Research Center, Ehime University, Japan. His current research is focused on lymphangiogenesis in tumor progression and cutaneous inflammation.

THE JOURNAL OF BIOLOGICAL CHEMISTRY VOL. 286, NO. 10, pp. 8055–8066, March 11, 2011

Angiopoietin-1/Tie2 Signal Augments Basal Notch Signal Controlling Vascular Quiescence by Inducing Delta-Like 4 Expression through AKT-mediated Activation of β-Catenin*[S]

Received for publication, October 12, 2010, and in revised form, December 27, 2010 Published, JBC Papers in Press, January 6, 2011, DOI 10.1074/jbc.M110.192641

Jianghui Zhang[‡], Shigetomo Fukuhara[‡1], Keisuke Sako[‡], Takato Takenouchi[§¶], Hiroshi Kitani[§], Tsutomu Kume[‖], Gou Young Koh[**], and Naoki Mochizuki[‡2]

From the [‡]Department of Cell Biology, National Cerebral and Cardiovascular Center Research Institute, Fujishirodai 5-7-1, Suita, Osaka 565-8565, Japan, the [§]Transgenic Animal Research Center, National Institute of Agrobiological Sciences, Ibaraki 305-8634, Japan, the [¶]Laboratory for Chemistry and Metabolism, Tokyo Metropolitan Institute for Neuroscience, Tokyo 183-8526, Japan, the [‖]Feinberg Cardiovascular Research Institute, Northwestern University, Chicago, Illinois 60611, and the [**]Biomedical Research Center and Department of Biological Sciences, Korea Advanced Institute of Science and Technology, Guseong-dong, Daejeon 305-701, Korea

Angiopoietin-1 (Ang1) regulates both vascular quiescence and angiogenesis through the receptor tyrosine kinase Tie2. We and another group previously showed that Ang1 and Tie2 form distinct signaling complexes at cell-cell and cell-matrix contacts. We further demonstrated that the former up-regulates Notch ligand delta-like 4 (Dll4) only in the presence of cell-cell contacts. Because Dll4/Notch signal restricts sprouting angiogenesis and promotes vascular stabilization, we investigated the mechanism of how the Ang1/Tie2 signal induces Dll4 expression to clarify the role of the Dll4/Notch signal in Ang1/Tie2 signal-mediated vascular quiescence. Under confluent endothelial cells, the basal Notch signal was observed. Ang1, moreover, induced Dll4 expression and production of the Notch intracellular domain (NICD). Ang1 stimulated transcriptional activity of β-catenin through phosphoinositide 3-kinase (PI3K)/AKT-mediated phosphorylation of glycogen synthase kinase 3β (GSK3β). Correspondingly, the GSK3β inhibitor up-regulated Dll4, whereas depletion of β-catenin by siRNA blocked Ang1-induced Dll4 expression, indicating the indispensability of β-catenin in Ang1-mediated up-regulation of Dll4. In addition, Dll4 expression by the GSK3β inhibitor was only observed in confluent cells, and was impeded by DAPT, a γ-secretase inhibitor, implying requirement of the Notch signal in β-catenin-dependent Dll4 expression. Consistently, we found that either Ang1 or NICD up-regulates Dll4 through the RBP-J binding site within intron 3 of the *DLL4* gene and that β-catenin forms a complex with NICD/RBP-J to enhance Dll4 expression. Ang1 induced the deposition of extracellular matrix that is preferable for basement membrane formation through Dll4/Notch signaling. Collectively, the Ang1/Tie2 signal potentiates basal Notch signal controlling vascular quiescence by up-regulating Dll4 through AKT-mediated activation of β-catenin.

Angiopoietin-1 (Ang1)[3] is a ligand for endothelium-specific receptor tyrosine kinase Tie2. Ang1/Tie2 signaling is essential for developmental vascular formation, as evidenced by the gene-targeting analyses of either Ang1 or Tie2 in mice (1–3). In quiescent adult vasculature, Ang1 secreted from mural cells induces Tie2 activation in endothelial cells to maintain mature blood vessels by enhancing vascular integrity and endothelial survival (4–6). Ang1/Tie2 signaling also plays an important role in physiological and pathological angiogenesis, as opposed to its function in quiescent vasculature (7–9). As to the dual functions of Ang1/Tie2 signaling, we and Saharinen *et al.* (11) have previously reported that Ang1 assembles distinct Tie2 signaling complexes in the presence or absence of endothelial cell-cell junctions, thereby regulating both vascular quiescence and angiogenesis (10). Ang1 induces *trans*-association of Tie2 in the presence of cell-cell contacts, whereas Tie2 is anchored to the cell-substratum contacts through extracellular matrix-bound Ang1 in the isolated endothelial cells. *Trans*-associated Tie2 and extracellular matrix-anchored Tie2 stimulate AKT and extracellular signal-regulated kinase 1/2 pathways preferable for vascular quiescence and angiogenesis, respectively.

By performing DNA microarray analyses, we have revealed that *trans*-associated Tie2, but not extracellular matrix-anchored Tie2, regulates the expression of genes involved in vascular quiescence, which include Krüppel-like factor 2, delta-

* This work was supported in part by grants from the Ministry of Education, Science, Sports and Culture of Japan (to S. F. and N. M.), the Ministry of Health, Labor, and Welfare of Japan (to N. M.), and the Program for the Promotion of Fundamental Studies in Health Sciences of the National Institute of Biomedical Innovation (to S. F. and N. M.), grants from the Naito Foundation (to S. F.), Takeda Science Foundation (to S. F. and N. M.), the Sagawa Foundation for Promotion of Cancer Research (to S. F.), Mochida Memorial Foundation for Medical and Pharmaceutical Research (to S. F.), Kowa Life Science Foundation (to S. F.), Kanae Foundation for the Promotion of Medical Science (to S. F.), The Novartis Foundation (Japan) for the Promotion of Science (to S. F.), Senri Life Science Foundation (to S. F.), the Mitsubishi Foundation (to N. M.), and a AstraZeneca Research Grant (to N. M.).

[S] The on-line version of this article (available at http://www.jbc.org) contains supplemental Figs. S1–S5.

[1] To whom correspondence may be addressed: Dept. of Cell Biology, National Cerebral and Cardiovascular Center Research Institute, 5-7-1 Fujishirodai, Suita, Osaka 565-8565, Japan. Tel.: 81-6-6833-5012; Fax: 81-6-6835-5461; E-mail: fuku@ri.ncvc.go.jp.

[2] To whom correspondence may be addressed. E-mail: nmochizu@ri.ncvc.go.jp.

[3] The abbreviations used are: Ang1, angiopoietin-1; Dll4, delta-like 4; VEGF, vascular endothelial growth factor; NICD, Notch intracellular domain; GSK3β, glycogen synthase kinase 3β; Ang2, angiopoietin-2; COMP, cartilage oligomeric matrix protein; DAPT, *N*-(*N*-(3,5-difluorophenacetyl)-L-alanyl)-*S*-phenylglycine *t*-butyl ester; HUVECs, human umbilical vein endothelial cells; CA-βCat, constitutively active mutant of β-catenin; CA-AKT, constitutively active mutant of AKT.

like 4 (Dll4), TIS11d, and connexin-40 (10). We have extended the studies on Ang1-mediated vascular quiescence and have shown that Ang1-induced Krüppel-like factor 2 expression occurs through the phosphoinositide 3-kinase (PI3K)/AKT pathway-mediated activation of myocyte enhancer factor 2, and counteracts vascular endothelial growth factor (VEGF)-mediated inflammatory responses (12).

Dll4 is a type 1 membrane protein belonging to the Delta/Serrate/Lag2 family of Notch ligands. Notch signaling is an evolutionally conserved pathway involved in cell fate specification during embryonic and postnatal development, and plays crucial roles in multiple aspects of vascular development such as arterial venous cell fate determination and tip/stalk cell specification during sprouting angiogenesis (13–15). Delta/Serrate/Lag2 ligands bind to Notch family receptors in a cell-cell contact-dependent manner, leading to cleavage of the Notch intracellular domain (NICD). NICD cleaved from Notch enters into the nucleus, associates with transcription factor RBP-J, and regulates the expression of Hes (Hairy/Enhancer of Slit) and Hey (Hes related with YRPW, also known as HesR, HRT and HERP) family of transcriptional repressors (16).

During the tip-stalk cell communication during sprouting angiogenesis, the Dll4/Notch signal is well characterized (17–21). VEGF up-regulates Dll4 expression in endothelial tip cells, which in turn leads to Notch activation in adjacent stalk cells. The stalk cells subsequently lose their responsiveness to VEGF through down-regulation of VEGF receptors such as VEGFR2 and Neuropilin-1 (22), thereby maintaining a quiescent and stabilized phenotype. Similarly, Dll4/Notch signaling is reported to be involved in tumor angiogenesis. In tumor vasculature, tumor-derived VEGF induces Dll4 expression in endothelial cells, which acts as a negative regulator of tumor angiogenesis, but is required for formation of functional vascular network (23–25). Indeed, blockade of Dll4/Notch signaling in tumor vasculature inhibits tumor growth by promoting non-productive angiogenesis associated with excessive sprouting from tumor vessels. The effect of Dll4/Notch signaling on tumor vasculature is reminiscent of that of Ang1/Tie2 signaling. Ang1/Tie2 signaling is also capable of inducing normalization of tumor vasculature by reducing excessive endothelial sprouting and promoting pericyte coverage (26–29).

The Notch signaling not only restricts angiogenesis but also maintains vascular quiescence (15, 30). It has been reported that conditional deletion of RBP-J, the key transcription factor downstream of the Notch receptor, induces spontaneous angiogenesis in quiescent adult vasculature (31). Similarly, Tie2 is activated in the endothelium of quiescent adult vasculature, and is believed to be involved in the maintenance of vascular quiescence (6, 32). Furthermore, both Ang1/Tie2 and Dll4/Notch signaling promote recruitment of mural cells to the vessel wall and induce deposition of basement membrane proteins around the vessels, both of which are important for vascular stabilization (26, 33–37).

Besides the role for the Dll4/Notch signal in the tip-stalk communication, the Dll4/Notch signal appears to function in mature blood vessels with tight interendothelial cell-cell contacts. Functional similarity between the Ang1/Tie2 signal and Dll4/Notch signal and our previous data that Ang1 induced Dll4 expression prompted us to test our hypothesis that the Ang1/Tie2 signal may promote vascular stabilization through the Dll4/Notch signal and to investigate how Dll4 is induced by Ang1/Tie2 signaling. In this study, we found that Ang1 induces activation of β-catenin through PI3K/AKT pathway-mediated inhibition of glycogen synthase kinase 3β (GSK3β) and that the stabilized β-catenin subsequently enhances Notch signal-induced Dll4 expression by forming a complex with NICD/RBP-J on the Dll4 intron3 enhancer, thereby potentiating the Dll4/Notch signal leading to vascular stabilization.

EXPERIMENTAL PROCEDURES

Reagents, Antibodies, and siRNAs—Ang1, angiopoietin-2, (Ang2), and cartilage oligomeric matrix protein (COMP)-Ang1 were prepared as described (38). Other reagents were purchased as follows: wortmannin, AKT inhibitor IV, and *N*-(*N*-(3,5-difluorophenacetyl)-L-alanyl)-*S*-phenylglycine *t*-butyl ester (DAPT) from Calbiochem; SB216763 from Sigma; lithium chloride (LiCl) from Wako Pure Chemical Industries; and basic fibroblast growth factor (bFGF) from PeproTech. Antibodies were purchased as follows: anti-Dll4, anti-cleaved Notch1 (Val^{1744}) (anti-NICD), anti-AKT, anti-phospho-AKT, anti-GSK3β, and anti-phospho-GSK3β (Ser^{9}) from Cell Signaling Technology; anti-tubulin from Sigma; anti-β-catenin from BD Biosciences; anti-RBP-J (K0043) from Tokusyu-meneki Laboratory; anti-collagen type IV from Millipore; rhodamine-phalloidin from Invitrogen Corp.; and horseradish peroxidase-coupled sheep anti-mouse and anti-rabbit IgG from GE Healthcare. Stealth small interfering RNAs (siRNAs) targeting the genes indicated were purchased from Invitrogen Corp.: human Dll4 (HSS123068, HSS182569) and human β-catenin (VHS50819, VHS50822).

Cell Culture, Transfection, siRNA-mediated Protein Knockdown, and Adenovirus Infection—Human umbilical vein endothelial cells (HUVECs) and human aortic endothelial cells were purchased from Kurabo, maintained as described previously (10, 39), and used for the experiments before passages 8 and 10, respectively. Human dermal microvascular endothelial cells were purchased from Kurabo, and maintained in HuMedia-MvG with a growth additive set. The cells were placed on collagen-coated plates at densities of 2,000 and 40,000 cells/cm^2, and cultured overnight to obtain sparse and confluent cell cultures, respectively. HUVECs were transfected using Lipofectamine 2000 (Invitrogen) and Lipofectamine Plus reagents (Invitrogen) according to the manufacturer's instructions. For siRNA-mediated gene silencing, HUVECs were transfected with 20 nM siRNA duplexes using Lipofectamine RNAi MAX reagent (Invitrogen), and cultured for 36–48 h. As a control, siRNA duplexes with irrelevant sequences were used. Then, the cells were harvested, re-plated on collagen-coated plates, and cultured for an additional 24 h before experiments. HUVECs were infected with adenovirus vectors at the appropriate multiplicity of infection. Forty-eight h after infection, the cells were used for experiments.

Plasmids and Adenoviruses—The DNA, including intron 3 of the human *DLL4* gene, was amplified by PCR using the genomic DNA extracted from HUVECs as a template and the following